



بِسْمِ اللَّهِ الرَّحْمَنِ الرَّحِيمِ

Sudan University of Science and Technology

College of Graduated Studies



**PERPRATION OF COPPER OXIDES
NANOSTRUCTURED VIA PULSED LASER
ABLATION IN LIQUIDS AND THEIR
CHARACTERIZATION**

**تحضير أكاسيد النحاس النانوية بواسطة الإستئصال الليزري في
السوائل وتوصيف خصائصها**

**A dissertation submitted as partial fulfillment of the
Requirements for the Degree of Master of Scince in
Physics**

Prepared By:

Nisrin Saeed Eljack

Supervised By:

Dr. Ali Abdel Rahman Saeed Marouf

March 2017

الآية الكريمة

قال تعالى(.....وعسى أن تكرهوا شيئا وهو خيرا لكم وعسى أن تحبوا شيئا
وهو شر لكم والله يعلم وأنتم لا تعلمون)

صدق الله العظيم

سورة البقرة اية (216)

DEDICATION

To my mother and father who inspire me to think,
dream and plan for a bright future

ACKNOWLEDGMENT

After praise and thanks for Almighty Allah (S.W.T) who gave me the health, ability and patience to accomplish this research, I would like to thank all people who helped and supported me to accomplish this thesis.

I want to thank Dr. Ali Marouf for his guidance and effort and patience and I want to thank my colleague Ammar Kamal master's student at the University Of King Fahd Of Petroleum & Minerals In Saudi Arabia, who is credited with God after the completion of the search.

Abstract

In present work, novel and one-step process, called Pulsed Laser Ablation in Liquids (PLAL) technique was used to synthesis a high purity, stable and less agglomeration nanostructure semiconductors.

Nanostructure copper oxides (cupric and cuprous oxides) were synthesized using Nd: YAG pulsed laser with wavelength of 532 nm. The effect of the oxidizing media on the composition, morphology and optical properties of the synthesized nanomaterials produced by PLAL were studied using XRD, EDS, FE-SEM, TEM, FTIR and UV-Vis spectrophotometer. The effect of annealing temperature on the synthesized nanostructure copper oxides in deionized water was also studied.

The results showed that the produced samples of Cu/Cu₂O nanostructure were converted predominantly into CuO nanostructure at annealing temperature of 300 °C. As the annealing temperature increases from 300 to 900 °C, the grain sizes of CuO nanostructure increased from 9 ± 1 to 26 ± 1 nm. The study revealed that the band gap and other optical properties of nanostructure Cu/Cu₂O were changed due to post annealing.

ملخص البحث

في هذا البحث تم استخدام تقنية فريدة وتتم في خطوة واحدة تسمى الاستئصال بالليزر النبضي في تقنية السوائل (PLAL)، لتخليق أشباه الموصلات نانوية التركيب عالية النقاء وأقل استقراراً.

تم تصنيع أكاسيد النحاس نانوية التركيب (النحاسيك والنحاسوز) باستخدام ليزر النيوديموم ياغ النبضي بطول موجي 532 نانومتر. تم دراسة تأثير الوسط المؤكسد على التركيب والمورفولوجيا والخصائص البصرية للمواد النانوية المصنعة من بتقنية (PLAL) باستخدام XRD و EDS و FE-SEM و TEM و UV-Vis spectrophotometer و FTIR. تمت دراسة تأثير درجة حرارة التلدين على أكاسيد النحاس النانوية المصنعة في الماء منزوع الأيونات. أظهرت النتائج أن (Cu/Cu₂O) الناتج تم تحويله في الغالب إلى CuO عند درجة حرارة تلدين 300 °C لمدة 3 ساعات. كلما زادت درجة حرارة التلدين من 300 إلى 900 درجة مئوية، زاد حجم الحبيبات من CuO من 1 ± 9 إلى 1 ± 26 نانومتر.

كشفت الدراسة أن فجوة الطاقة وخصائص بصرية أخرى لتركيب كل من النحاسيك والنحاسوز

النانوية تغيير بتغير في درجة الحرارة

TABLE OF CONTENTS

الاية	II
DEDICATION.....	III
ACKNOWLEDGMENT.....	IV
ABSTRACT.....	V
ABSTRACT (ARABIC) ملخص البحث	VI
TABLE OF CONTENTS.....	VII
LIST OF FIGURES.....	X
Chapter One Introduction and Literature Review	
1.1Introduction.....	1
1.2 Research ProblemStatement.....	2
1.3Literature Review.....	2
1.3.1 copper Oxides Nanoparticles.....	3
1.4 Objectives.....	5
1.5 ThesisLayout.....	6
Chapter Two Theoretical Background	
2.1Inroduction.....	7
2.2 Classification Of Nanomaterials	8
2.2.1 Zero-Dimensional Nanomaterials.....	8
2.2.2 One-Dimensional Nanomaterials.....	9
2.2.3 Two-Dimensional Nanomaterials.....	9
2.2.4 Three-Dimensional Nanomaterials.....	9
2.3 Properties of Nanomaterials.....	10
2.3.1 Optical Properties.....	11
2.3.2 Electrical Properties.....	12
2.3.3 Mechanical Properties.....	12
2.3.4 Magnetic Properties.....	14
2.4 Approaches to The Synthesis Of Nanomaterials.....	14
2.4.1 Bottom-Up Approach.....	15

2.4.2 Top-Down Approach.....	15
2.5 Laser	16
2.5.1 Basic Construction and Principle Of Lasing.....	16
2.5.2 Population Inversion.....	17
2.5.3 Elements of Laser.....	18
2.5.4 Properties of Laser Light.....	20
2.5.5 Laser Classification.....	22
2.5.6 Pulsed Laser Ablation (PLA)	26
2.5.7 Fundamentals of Interaction Of The Laser Beam With The Matter.....	27
3 CHAPTER THREE METHODOLGY AND CHARACTERIZATION	
3.1 The Tools.....	32
3.2 Experimental Setup for Synthesis of Nanoparticles (NPs(.....	33
3.3 Characterization Techniques for Synthesized Nanoparticles.....	38
3.3.1 X-ray Diffraction (XRD).....	38
3.3.2 Field Emission Scanning Electron Microscopy (FE-SEM)	39
3.3.3 UV-Vis Spectrophotometer for Band Gap Measurements	40
3.3.4 Spectrofluorometer for Photoluminescence Study	41
4 CHAPTER FOUR RESULTS AND DISCUSSIONS	
4.1 Synthesis of Copper Oxides NPs.....	42
4.1.1 Effects of Oxidizing Medium	42
4.1.1.1 Structure and Morphology of Synthesized Material.....	44
4.1.1.2 Optical Characterization of the synthesized Material	50
4.1.2 Effects of Annealing Temperature	56
4.1.2.1 Structure and Morphology of unannealed/annealed Copper oxides NPs ...	57
4.1.2.2 Effect of annealing temperature on grain size.....	60
4.1.2.3 Optical Characterization of unannealed/ annealed copper oxide NPs.....	63
4.2 CONCLUSIONS	65
4.3 Recommendations.....	66
REFERENCES.....	67

LIST OF FIGURES

Fig 2-1 Illustrates Bottom-up and the top-down approaches in synthesis of nanomaterials	16
Fig 2.2 Elements of laser	18
Fig 2.3 Incoherent light waves	21
Fig 2.4 Coherent light waves	21
Fig 2.5 He Ne laser	23
Fig 2.6 show Nd: YAG laser	26
Fig 2.7 PLS systems where a focused beam irradiates	27
Fig 3.1 photograph of the Nd:YAG laser at laser Laboratory of KFUPM	32
Fig 3.2 The Target - metallic copper	33
Fig 3-3 Schematic diagram of the focusing arrangement of the setup for synthesis of nanostructured semiconductors from solid target using PLAL technique	34
Fig 3-4 Photograph of PLAL setup developed at Laser Laboratory of KFUPM	35
Fig 3-5 Photographs of the essential parts in PLAL	36
Fig 3-6 Photograph of the glass cell and the magnetic rotator with different volumes of liquid.	37
Fig 3-7 photographs of different designs of magnetic rotator	38
Fig 3-8 Photograph of the X-ray diffractometer used in this study	39
Fig 3-9 Photograph of FE-SEM and EDS systems used in this work.	40
Fig 3-10 Photograph of UV-Vis spectrophotometer used in this work	40
Fig 3-11 Photograph of Spectrofluorometer used in this work.	42
Fig 4-1. The appearance and color of the synthesized nanomaterial samples by varying the concentrations of H ₂ O ₂ in the DW as indicated in the figure.	44
Fig 4-2 EDS spectrum of the synthesized nanomaterial in 0 % of H ₂ O ₂ in the DW as indicated on the figure.	44
Fig 4-3 EDS spectrum of the synthesized nanomaterial in 1 % of H ₂ O ₂ in the DI water as indicated on the figure.	45
Fig 4-4 EDS spectrum of the synthesized nanomaterial in 3 % of H ₂ O ₂ in the DW as indicated on the figure.	45
Fig 4-5 EDS spectrum of the synthesized nanomaterial in 5 % of H ₂ O ₂ in the DW as indicated on the figure.	46
Fig 4-6 X-ray diffraction of the synthesized nanomaterial in 0 % of H ₂ O ₂ in the DW.	46
Fig 4-7 X-ray diffraction of the synthesized nanomaterial in 1 % of H ₂ O ₂ in the DW.	47
Fig 4-8 X-ray diffraction of the synthesized nanomaterial in 3 % of H ₂ O ₂ in the DW.	47
Fig 4-9 X-ray diffraction of the synthesized nanomaterial in 5 % of H ₂ O ₂ in the DW.	48
Fig 4-10 TEM image of the synthesized nanomaterial in 0% of H ₂ O ₂ in the DW.	49
Fig 4-11 TEM image of the synthesized nanomaterial in 5% of H ₂ O ₂ in the DW.	49
Fig 4-12. Absorption spectrum of synthesized nanomaterial in 0 % of H ₂ O ₂ in the DW.	50
Fig 4-13 Absorption spectrum (A) of synthesized nanomaterial in 1 % of H ₂ O ₂ in the DI water. The Gaussian Peak fit is shown in (B), (C) and (D).	51
Fig 4-14 Absorption spectrum (A) of synthesized nanomaterial in 3 % of H ₂ O ₂ in the DI water. The Gaussian Peak fit is shown in (B), (C) and (D).	51
Fig 4-15 Absorption spectrum (A) of synthesized nanomaterial in 5 % of H ₂ O ₂ in the DW. The Gaussian Peak fit is shown in (B), (C) and (D).	52

Fig 4-16 Tauc plot of the synthesized nanomaterial in 0 % of H₂O₂ in the DW.	54
Fig 4-17 Tauc plot of the synthesized nanomaterial in 1 % of H₂O₂ in the DW.	55
Fig 4-18 Tauc plot of the synthesized nanomaterial in 3 % of H₂O₂ in the DW.	55
Fig 4-19 Tauc plot of the synthesized nanomaterial in 5 % of H₂O₂ in the DW.	56
Fig 4-20 X-ray diffraction of Cu/Cu₂O prepared by pulsed laser ablation in DW.	57
Fig 4-21 XRD patterns of CuO prepared by annealing Cu/Cu₂O at 300 °C for three hours.	58
Fig 4-22 XRD patterns of CuO prepared by annealing Cu/Cu₂O at 600 °C for three hours.	58
Fig 4-23 XRD patterns of CuO prepared by annealing Cu/Cu₂O at 900 °C for three hours.	59
Fig 4-24 TEM image of unannealed Cu/Cu₂O sample	61
Fig 4-25 TEM image of annealed Cu/Cu₂O sample at 600°C.	62
Fig 4-26 TEM image of annealed Cu/Cu₂O sample at 900°C.	62
Fig 4-27 Absorption spectra of Cu/Cu₂O nanoparticles prepared by laser ablation of Copper in DW.	63
Fig 4-28 Tauc's plot of as-prepared material.	64

CHAPTER ONE

Introduction and Literature Review

1.1 INTRODUCTION

Pulsed laser ablation (PLA) was first developed in the 1960s, shortly after the invention of the pulsed ruby laser. Since then, laser ablation in a vacuum or dilute gas has been studied by many researchers. By using different target materials and background gases, and varying parameters such as the laser wavelength, fluence, and pulse duration, it is possible to produce a wide variety of thin films. These include high temperature superconductors (Dijkkamp D et al 1987), metals, semiconductors, oxides, and other ceramics (Radhakrishnan G, Adams P M 1999), and diamond-like carbon (Pappas D L et al 1992). The thin films have a variety of applications, for example semiconductor devices, electrodes, and wear-resistant coatings (Loir A S et al 2004).

The introduction of pulsed laser ablation at the solid-liquid interface was first reported by Patil and co-workers in 1987, who used a pulsed laser to ablate a pure iron target in water to form iron oxides with metastable phases (Patil P P et al 1987). This method is known as Liquid Phase Pulsed Laser Ablation (LP-PLA), in which a solid target is immersed in a liquid medium and the laser beam is focused through the liquid onto the target surface. Following their work, (Ogale S B 1988) extended the potential of LP-PLA for the surface modification of metals, such as metallic oxidation, nitriding, and carbiding. This pioneering work opened new routes for materials processing based on the PLA of solids in various liquids. Since then, the LP-PLA method has been used to produce a wide range of novel materials, such

as nanodiamond and related nanocrystals, metallic nano crystals, nanocrystal alloys, and metal oxides. These studies clearly indicate that LP-PLA has become a successful material fabrication technique, allowing versatile design through choosing suitable solid targets and confining liquids. Compared to the conventional physical methods (including chemical vapour deposition (Kempa K et al 2003), vapour phase transport (Duan X F, Lieber C M 2000) and pulsed laser ablation in vacuum (Sun Y et al 2005), and chemical methods (Yang H G, Zeng H C 2004) (including hydrothermal methods, soft-template (Mirkin C A et al 1996) and use of various surfactants (Sun Y G et al 2002), the technique of LP-PLA has many distinct advantages. These include (i) a chemically 'simple and clean' synthesis, the final product is usually obtained without byproducts and no need for further purification; (ii) low cost of experimental setup and easily controlled parameters; (iii) the extreme confined conditions and induced high Temperature, high pressure region favour the formation of unusual metastable phases. These advantages allow the designer to combine selected solid targets and liquid to fabricate compound nanostructures with desired functions.

1.2 Research Problem Statement

Synthesis of material in nano-scale using the pulsed laser ablation technique.

1.3 LITERATURE REVIEW

The main aim of this section is to summarize the recent published literature which have attracted great attention on development of PLAL technique and using it to synthesize the copper oxides nanoparticles.

In 1993 the possibility of this technique to synthesize colloidal solutions

of metallic target in the presence of organic solvents and water was reported by Neddersen et al (Yan, Z. and Chrisey, D.B, 2012). In the early 2000s, researchers started to generate and control the size of nanostructured noble metals by pulsed laser ablation in the presence of aqueous solutions and surfactants. Since then, PLAL has been applied to synthesize a wide variety of nanostructured materials which gained high popularity as these methods allow one to obtain nanomaterial with a high degree of purity (as laser beams being a completely clean tool) and one can ablate nearly all kinds of materials, as laser beam possesses high power density after focusing (Yang, G. ed., 2012) (Liu, P et al 2010)

1.3.1 Copper Oxides Nanoparticles

Transition metals show unique characteristics like existence of various oxidation states, formation of paramagnetic compounds, high melting point, high boiling point, effective homogeneous and heterogeneous catalytic activity and all these properties can be ascribed to the partially filled d shells. Transition metal oxides form a series of compounds with a wide range of unique electronic properties and they have important phases such as dielectrics, semiconductors and metals, and could be utilized very well as materials for magnetic, electrochromic, optical and catalytic applications (Devan R.S 2012). The advent of the nanostructured material has brought about the improved attributes in terms of magnetic, electronic, catalytic, sensing and optical characteristics compared to their bulk counterparts (Link, S. and El-Sayed, M.A., 1999) (Lee, J et al 2006). Copper oxide is one of the most extensively studied transition metal oxides and finds widespread applications as well. The predominant oxides of copper are cupric oxide or Copper (II) oxide (CuO) and cuprous oxide or Copper (I) oxide (Cu₂O), ignoring the presence of other forms of oxides which are quite

marginal. From application point of view, CuO is more versatile than Cu₂O, where the former is widely applied in the fields of solar energy conversion, nano-fluid and gas sensors, (Chowdhuri, Aet al 2003)(Chang, M.H et al 2011).and the latter is mostly applied in the areas of bacterial disinfection (Gopalakrishnan, K 2012) and solar cells (Rai, B.P., 1988). Both CuO and Cu₂O are p-type semiconductors possessing monoclinic and cubic crystal structures respectively and the band gap energy for CuO is in the range of 1.2 to 2.1 eV while for Cu₂O is in the range of 2.1 to 2.6 eV. These variations are quite evident in the published literature (Yoon, K.H et al 2000).Yeh et al studied the production of Cu NPs by PLA of suspended CuO powder in 2-propanol usingNd: YAG nanosecond laser operating either at 1064 or 532 nm of wavelength (Yeh M S et al 1999).Amikura et al reported the synthesis of Cu₄O₃and Cu NPs using PLAL. In this study, Nd: YAG nanosecond laser (532 nm wavelength, 6 ns pulsed duration and operating at 184-210 mj/Pulse of energy) was applied to ablate Cu plate in DW and decane to synthesize Cu₄O₃and Cu NPs respectively (Amikura K, et al 2008). Lin et al used PLAL (532 nm wavelength, focused nanosecond laser (10 ns), 5Hz repetition rate, 100 mj/pulse energy and 60minutes ablation time) to synthesize CuOnanorod from the ablation of Cu target in DW. By applying electric field during the ablation and without focusing, the authors were able to synthesize spin-like CuO(Lin X,Z et al 2009).

Lee et al produced spin-like CuO and Cu NPs using 532nm from Nd: YAG nanosecond laser (4-6 ns pulse duration and 8.9 mj/cm² energy density) for the ablation of suspended CuO powder in methanol(Lee et al 2009). Niu et al produced Cu nanowires using 1064 nm from Nd: YAG laser (1 ms pulse duration, 20 Hz pulse repetition, 10⁶W/cm² laser fluence and for 5 min ablation time) to ablate Cu target in 1-Dodecanethiol (Niu

et al 2010). The authors were able to synthesis hollow CuO NPs from the ablation of Cu plate in water + ethanol using Nd: YAG laser (1064 nm, 0.6 ms pulse duration, 1 Hz pulse repetition, 106 W/cm^2 laser fluence and 5 min ablation time)(Niu et al 2010).

Nath and Khare used Nd: YAG nanosecond laser (532 nm, 10 ns) to ablate Cu plate in DW. By changing the focusing condition to adjust the energy density, CuO NPs ($\leq 200 \text{ nm}$), CuO/Cu₂O and Cu/Cu₂O composites were synthesized at 500 J/cm^2 , 80 J/cm^2 and 9 J/cm^2 respectively (Nath and Khare 2011). Kawasakisynthesized Cu NPs (10 nm) using pulsed laser ablation (164 nm) from suspended CuO powder in acetone . The as prepared Cu NPs were converted into Cu₂O NPs by oxidation process in the open air(Kawasaki M 2011).Muniz-Miranda et alused PLAL to synthesize from Cu colloidal suspensions. The authors used Nd: YAG laser (1064 or 532 nm, 10 ns pulse duration, 10 Hz pulse repetition, 2.5 mj/cm^2 energy density and 10-30 min ablation time)as ablation source to synthesize Cu colloidal suspensions by the ablation of Cu plate in aqueous solution. (Muniz-Miranda, M et al 2011). However there is no authentic report or published data regarding the effect of oxidizing medium and annealing temperature on theproperties of copper oxide nanoparticles using PLAL technique. Hence, the work in this direction could be considered as a pioneer work.

1.4 Objectives

The main objective of this thesis is to synthesize ultrafine nanostructured semiconductors using pulsed laser ablation in liquid. The specific objectives are the following:

1. To design a homemade set up that could improve and achieve efficient conditions for pulsed laser ablation in liquids.

2. To synthesize Cu_2O , CuO nanoparticles using pulsed laser ablation in liquid technique.
3. To characterize the synthesized nanoparticles using different analytical techniques.

1.5 Thesis Layout

This thesis is consist of four chapters, chapter one Introduction and Literature Review ,and chapter tow consist Basic Concepts of laser, and Light interaction with matter, chapter three consist Experimental Part (The materials and device and method), chapter four consist Results and Discussion and Conclusion, Recommendations and Refrence.

CHAPTER TWO

Theoretical Background

2.1 INTRODUCTION

The fabrication of devices at atomic and molecular scale was predicted by physicist Richard Feynman in his famous talk entitled “There’s plenty of room at the bottom” at an American Physical Society meeting on December 29th, 1959 (Feynman, R.P 1961) . The prefix “nano” has found in last decade an ever-increasing application to different fields of the knowledge. The prefix comes from the ancient Greek νᾶνος through the Latin nanus meaning literally dwarf and, by extension, very small. The term “Nanotechnology” was coined by Professor Norio Taniguchi at the University of Tokyo and it has been in use as early as 1974(Taniguchi, N 1974). Nanotechnology is a technology which deals with different structures of matter of the order of 10^{-9} of a meter. In 2006, Nanotechnology was defined by the US National Nanotechnology Initiative as follows: “Nanotechnology is development at the atomic levels in the length scale of approximately 1-100 nanometer range, to provide a fundamental understanding of phenomena and materials at the nanoscale and to create and use structures, devices and systems that have novel properties and functions”(Ba, J.H 2006). The term “nano” refers to a billionth (10^{-9}) The term “Nanomaterials” refers to a ultrafine parts of the material where at least one of its dimensions is in nanometer scale (from 1nm to 100 nm). The nanomaterials are classified according to the dimensions (Zero dimension, One dimension, Two dimension and Three dimension).The nanomaterials have a unique properties will be presented in this chapter. The invention and

development of high resolution imaging tools such as the scanning tunneling microscope (STM), atomic force microscope (AFM), transmission electron microscope (TEM) and scanning electron microscope (SEM) play an important role in the characterization of nanomaterials and advancement of nanoscience.

Nanomaterials show different physical and chemical properties from that of its bulk counterparts. These unique characteristics arise due to the quantum confinement and the increase of surface area to volume ratio which are inversely proportional to particle size (Poole Jr, C.P. and Owens, F.J., 2003). Hence, synthesis and application of nanomaterials have attracted great attention from researchers for their applications in different areas such as sensing, energy harvesting and photo-catalysis. Several methods have been applied to synthesize nanomaterials such as wet chemical synthesis, vapor phase condensation, rapid thermal decomposition of precursors in solution, sputtering and plasma reactors. Some of these methods, especially the chemical methods, are capable of producing large quantities, but they typically require many steps (pretreatment, mixing, chemical reaction, filtration, drying and heat-treatment). Such treatments may alter the material purity, promote grain growth, and introduce contaminants. Purification of such contamination to obtain nanomaterial with a high degree of purity could add extra cost

2.2 Classification of Nanomaterials

Nanomaterials have extremely small size which having at least one dimension 100 nm or less. Nanomaterials can be classified according to the number of dimensions, it can be nanoscale in one dimension (eg. surface films), two dimensions (eg strands or fibres), or three dimensions (eg. Particles) .

2.2.1 Zero-dimensional nanomaterials:

Materials where in all the dimensions are measured within the nanoscale (no dimensions, or 0-D, are larger than 100 nm). The most common representation of zero-dimensional nanomaterials are nanoparticles. Nanoparticles can be amorphous or crystalline, it can be single crystalline or polycrystalline also it can be composed of single or multi-chemical elements. (Mokero, V.G et al, 2001)

2.2.2 One-dimensional nanomaterials:

Materials where in two dimensions in nanoscale one dimension that is outside the nanoscale. This leads to needle like-shaped nanomaterials. 1-D materials include nanotubes, nanorods, and nanowires. 1-D nanomaterials can be Amorphous or crystalline. It can be Single crystalline or polycrystalline, also it can be chemically pure or impure.

2.2.3 Two-dimensional nanomaterials:

Two of the dimensions are not confined to the nanoscale. 2-D nanomaterials exhibit plate-like shapes. Two-dimensional nanomaterials include nanofilms, nanolayers, and nanocoatings. 2-D nanomaterials can be Amorphous or crystalline, it can be made up of various chemical compositions, used as a single layer or as multilayer structures and it can be deposited on a substrate.

2.2.4 Three-dimensional nanomaterials:

Bulk nanomaterials are materials that are not confined to the nanoscale in any dimension. These materials are thus characterized by having three arbitrarily dimensions above 100 nm. Materials possess a nano crystalline structure or involve the presence of features at the nanoscale .

In terms of nano crystalline structure, bulk nanomaterials can be composed of a multiple arrangement of nanosize crystals, most typically in different orientations. With respect to the presence of features at the nanoscale, 3-D nanomaterials can contain dispersions of nanoparticles, bundles of nanowires, and nanotubes as well as multinanolayers.

2.3 Properties of Nanomaterials

Nanomaterials have the structural features in between of those of atoms and the bulk materials. While most microstructured materials have similar properties to the corresponding bulk materials, the properties of materials with nanometer dimensions are significantly different from those of atoms and bulks materials. This is mainly due to the nanometer size of the materials which render them: (i) large fraction of surface atoms; (ii) high surface energy; (iii) spatial confinement; (iv) reduced imperfections, which do not exist in the corresponding bulk materials. Due to their small dimensions, nanomaterials have extremely large surface area to volume ratio, which makes a large to be the surface or interfacial atoms, resulting in more “surface” dependent material properties. Especially when the sizes of nanomaterials are comparable to length, the entire material will be affected by the surface properties of nanomaterials. This in turn may enhance or modify the properties of the bulk materials. For example, metallic nanoparticles can be used as very active catalysts. Chemical sensors from nanoparticles and nanowires enhanced the sensitivity and sensor selectivity. The nanometer feature sizes of nanomaterials also have spatial confinement effect on the materials, which bring the quantum effects. The energy band structure and charge carrier density in the materials can be modified quite differently from their bulk and in turn will modify the electronic and optical properties of the materials. For example, lasers and light emitting diodes (LED) from both of the

quantum dots and quantum wires are very promising in the future optoelecton. High density information storage using quantum dot devices is also a fast developing area. Reduced imperfections are also an important factor in determination of the properties of the nanomaterials. Nanostructures and Nanomaterials favors of a selfpurification process in that the impurities and intrinsic materialdefects will move to near the surface upon thermal annealing. This increased materials perfection affects the properties of nanomaterials. For example, the chemical stability for certain nanomaterials may be enhanced, the mechanical properties of nanomaterials will be better than the bulk materials. The superior mechanical properties of carbon nanotubes are well known. Due to their nanometer size, nanomaterials are already known to have many novel properties. Many novel applications of the nanomaterials rose from these novel properties have also been proposed.

2.3.1 Optical properties:

One of the most fascinating and useful aspects of nanomaterials is their optical properties. Applications based on optical properties of nanomaterials include optical detector, laser, sensor, imaging, phosphor, display, solar cell, photocatalysis, photoelectron chemistry and biomedicine. The optical properties of nanomaterials depend on parameters such as feature size, shape, surface characteristics, and other variables including doping and interaction with the surrounding environment or other nanostructures. Likewise, shape can have dramatic influence on optical properties of metal nanostructures.

2.3.2 Electrical properties:

Electrical Properties of Nanoparticles” discuss about fundamentals of electrical conductivity in nanotubes and nanorods, carbon nanotubes, photoconductivity of nanorods, electrical conductivity of nanocomposites. One interesting method which can be used to demonstrate the steps in conductance is the mechanical thinning of a nanowire and measurement of the electrical current at a constant applied voltage. The important point here is that, with decreasing diameter of the wire, the number of electron wave modes contributing to the electrical conductivity is becoming increasingly smaller by well-defined quantized steps.

In electrically conducting carbon nanotubes, only one electron wave mode is observed which transport the electrical current. As the lengths and orientations of the carbon nanotubes are different, they touch the surface of the mercury at different times, which provides two sets of information: (i) the influence of carbon nanotube length on the resistance; and (ii) the resistances of the different nanotubes. As the nanotubes have different lengths, then with increasing protrusion of the fiber bundle an increasing number of carbon nanotubes will touch the surface of the mercury droplet and contribute to the electrical current transport.

2.3.3 Mechanical properties:

“Mechanical Properties of Nanoparticles” deals with bulk metallic and ceramic materials, influence of porosity, influence of grain size, superplasticity, filled polymer composites, particle-filled polymers, polymer-based nanocomposites filled with platelets, carbon nanotube-based composites. The discussion of mechanical properties of nanomaterials is, in to some extent, only of quite basic interest, the reason being that it is problematic to produce macroscopic bodies with a high

density and a grain size in the range of less than 100 nm. However, two materials, neither of which is produced by pressing and sintering, have attracted much greater interest as they will undoubtedly achieve industrial importance.

These materials are polymers which contain nanoparticles or nanotubes to improve their mechanical behaviors, and severely plastic-deformed metals, which exhibit astonishing properties. However, because of their larger grain size, the latter are generally not accepted as nanomaterials. Experimental studies on the mechanical properties of bulk nanomaterials are generally impaired by major experimental problems in producing specimens with exactly defined grain sizes and porosities. Therefore, model calculations and molecular dynamic studies are of major importance for an understanding of the mechanical properties of these materials. Filling polymers with nanoparticles or nanorods and nanotubes, respectively, leads to significant improvements in their mechanical properties. Such improvements depend heavily on the type of the filler and the way in which the filling is conducted. The latter point is of special importance, as any specific advantages of a nanoparticulate filler may be lost if the filler forms aggregates, thereby mimicking the large particles. Particulate filled polymer-based nano composites exhibit a broad range of failure strengths and strains. This depends on the shape of the filler, particles or platelets, and on the degree of agglomeration. In this class of material, polymers filled with silicate platelets exhibit the best mechanical properties and are of the greatest economic relevance. The larger the particles of the filler or agglomerates, the poorer are the properties obtained. Although, potentially, the best composites are those filled with nanofibers or nanotubes, experience teaches that sometimes such composites have the least ductility. On the other hand, by using

carbon nanotubes it is possible to produce composite fibers with extremely high strength and strain at rupture. Among the most exciting nanocomposites are the polymer/ceramic nanocomposites, where the ceramic phase is platelet-shaped. This type of composite is preferred in nature, and is found in the structure of bones, where it consists of crystallized mineral platelets of a few nanometers thickness that are bound together with collagen as the matrix. Composites consisting of a polymer matrix and defoliated phyllosilicates exhibit excellent mechanical and thermal properties.

2.3.4 Magnetic properties:

Bulk gold and Pt are non-magnetic, but at the nano size they are magnetic. Surface atoms are not only different to bulk atoms, but they can also be modified by interaction with other chemical species, that is, by capping the nanoparticles. This phenomenon opens the possibility to modify the physical properties of the nanoparticles by capping them with appropriate molecules. Actually, it should be possible that non-ferromagnetic bulk materials exhibit ferromagnetic-like behavior when prepared in nano range.

2.4 Approaches to the Synthesis of Nanomaterials

There are two major approaches in synthesizing nanomaterials: bottom-up or top-down. Depending on the experimental conditions employed, the properties and structure of the synthesized nanoparticles can be controlled. Routes for the synthesis of nanoparticles allows the control the particle size, particle geometry, doping ratio by different elements, and degree of particle agglomeration. Those particle parameters give the synthesized material new physical and chemical properties for different applications. A deep understanding of the synthetic

approach is critical in order to manufacture new structures with unique properties. Many techniques have been reported regarding both approaches such as chemical vapor deposition, sol gel, PLS, sputtering, mechanical milling and other techniques . In this research we are just focusing on those techniques that use pulsed laser techniques. The schematic shown in Fig (2-1).

2.4.1 Bottom-Up approach

Many nanomaterials are synthesized by the interaction of atoms or/and some molecular species through a set of chemical reactions provided by the technique . The precursor is typically a liquid or gas that is ionized, dissociated, sublimated or evaporated and then condensed to form either an amorphous or/and crystalline nanoparticle. This approach produces nanoparticles with fewer defects, homogenous chemical composition, less contamination, and particles with a narrow size distribution.

2.4.2 Top-Down approach

The starting material is a bulk material of the same material to be synthesized, which is then broken into smaller and smaller fragments or particles when a source of energy is applied. The energy applied can be mechanical, chemical or thermal, or could be another form of energy such as laser irradiation. In Pulsed Laser Ablation (PLA) and Pulsed Laser Deposition (PLD), the energy is absorbed by the material and transformed into chemical and/or thermal. energy to break (inter) molecular bonds of the bulk material . This approach usually results in smaller flakes or particles with a wide size distribution.

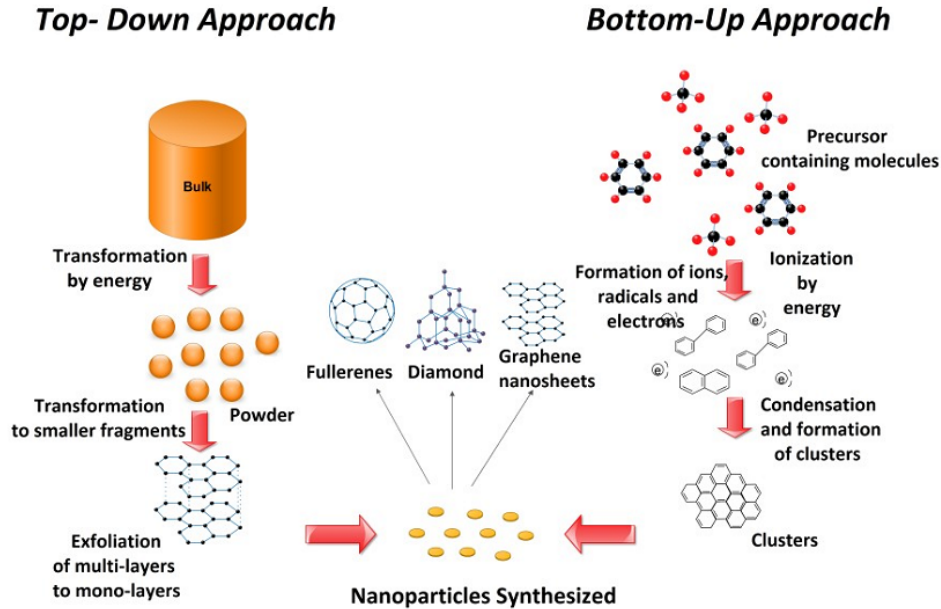


Fig (2-1) Illustrates Bottom-up and the top-down approaches in synthesis of nanomaterial

In this research we are adopted this technique represented in The Pulsed Laser Ablation (PLA) but firstly, we will talk about a LASER.

2.5 LASER

The term "laser" originated as an acronym for "light amplification by stimulated emission of radiation" "Laser is a powerful source of light having extraordinary properties which are not found in the normal light source like tungsten lamps or mercury lamps, etc. The unique property of laser is that wave travel very long distances with very little divergence.(Singh, S.C et al, 2012)

2.5.1 Basic Construction and Principle of Lasing

Basically, any laser system essentially has an active/gain medium, placed between a pair of optically parallel and highly reflecting mirrors with one of them partially transmitting, and an energy source to pump active

medium. The gain media may be solid, liquid, or gas and have the property to amplify the amplitude of the light wave passing through it by stimulated emission, while pumping may be electrical or optical. The gain medium used to place between pair of mirrors in such a way that light oscillating between mirrors passes every time through the gain medium and after attaining considerable amplification emits through the transmitting mirror. Let us consider an active medium of atoms having only two energy levels: excited level E_2 and ground level E_1 . If atoms in the ground state, E_1 , are excited to the upper state, E_2 , by means of any pumping mechanism (optical, electrical discharge, passing current, or electron bombardment), then just after few nanoseconds of their excitation, atoms return to the ground state emitting photons of energy $h\nu = E_2 - E_1$. According to Einstein's 1917 theory, emission process may occur in two different ways, either it may induced by photon or it may occur spontaneously. The former case is termed a stimulated emission, while the latter is known a spontaneous emission. Photons emitted by stimulated emission have the same Frequency, phase, and state of polarization as the stimulating photon; therefore they add to the wave of stimulating photon on a constructive basis, thereby increasing its amplitude to make lasing. At thermal equilibrium, the probability of stimulated emission is much lower than that of spontaneous emission ($1:10^{33}$) therefore most of the conventional light sources are incoherent, and only lasing is possible in the conditions other than the thermal equilibrium. The main condition for produce laser it is population inversion

2.5.2 POPULATION INVERSION

The number of atoms in any level at given time is called the population of that level. Normally, when the material is not excited extremely, the

population of the lower level or ground state is greater than that of upper level. When the population of upper level exceeds that of lower level, which is a reversal of the normal occupancy, the process is called population inversion. The situation is essential for a laser action. For any stimulated emission, It is necessary that the upper energy level or metastable state should have a long life time, i.e, the atoms should pause at the metastable state for more time than at the lower level. Thus, for laser action, pumping mechanism (exciting with external source) is necessary to maintain a higher population of atoms in the upper energy level relative to that in the lower level.

2.5.3 ELEMENTS OF LASER

In any system laser of there must be four functional elements are necessary in lasers to produce coherent light by stimulated emission of radiation. Fig (2.2) illustrates these four functional elements.

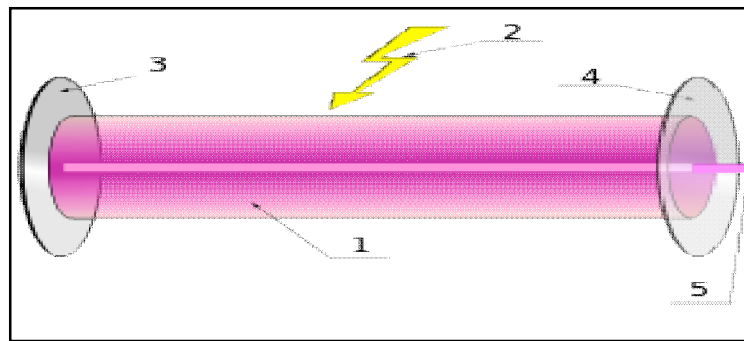


Fig (2.2) Elements of laser

- 1- Active Medium 2- Excitation Mechanism 3- Feedback Mechanism**
- 4- Output Coupler (OC) 5- Laser Beam**

2.5.3.1 ACTIVE MEDIUM

The active medium is collection of atoms or molecules that can be excited to a state of inverted population; that is, where more atoms or molecules

are in an excited state than in some lower energy state. The two states chosen for the lasing transition must possess certain characteristics. First, atoms must remain in the upper lasing level for a relatively long time to provide more emitted photons by stimulated emission than spontaneous emission. Second, there must be an effective method of "pumping" atoms from the highly-populated ground state into the upper lasing state in order to increase the population of the higher energy level over the population lower energy level. An increase in population of the lower energy level to a number above that in the high energy level will negate the population inversion and thereby prevent the amplification of emitted light by stimulated emission. In other words, as atoms move from the upper energy level to the lower energy level, more photons will be lost by spontaneous emission ___ giving off randomly directed, out-of-phase light ___ than gained due to the process of stimulated emission.

The active medium of a laser can be thought of as an optical amplifier. A beam of coherent light entering one end of the active medium is amplified through stimulated emission until a coherent beam of increased intensity leaves the other end of the active medium. Thus, the active medium provides optical gain in the laser. The active medium may be a gas, a liquid, a solid material, or a junction between two slabs of semiconductor.

2.5.3.2 EXCITATION MECHANISM

The excitation mechanism is a source of energy that excites, or "pumps" the atoms in the active medium from a lower to a higher energy state in order to create a population inversion. In gas laser and semiconductor lasers, the excitation mechanism usually consists of an electrical –current flow through the active medium. Solid and liquid lasers most often employ optical pumps.

2.5.3.3 FEEDBACK MECHANISM

The feedback returns a portion of the coherent light originally produced in the active medium for further amplification by stimulated emission. The amount of coherent light produced by stimulated emission depends upon both the degree of population inversion and strength of the stimulating signal. The feedback mechanism usually consists of two mirrors one at each end of the active medium, aligned in such a manner that they reflect the coherent light back and forth through the active medium.

2.5.3.4 OUTPUT COUPLER

The output coupler allows a portion of the laser light contained between the two mirrors to leave the laser in the form of a beam. One of the mirrors of the feedback mechanism allows some light to be transmitted through it at the laser wavelength. The fraction of the coherent light allowed to escape varies greatly from one laser to another from less than one percent for some helium-neon lasers to more than 80 percent for many solid-state lasers.

2.5.4 PROPERTIES OF LASER LIGHT

Light produced from the lasers have several valuable characteristics not shown by light obtained from other conventional light sources, which make them suitable for a variety of scientific and technological applications.

2.5.4.1 Coherence:

is one of the striking properties of the laser light and distinguishes it from the light from other sources. The basic meaning of coherence is that all

the waves in the laser beam remain spatially and temporarily in the same phase. Fig (2.3)

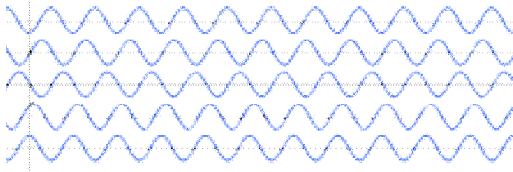
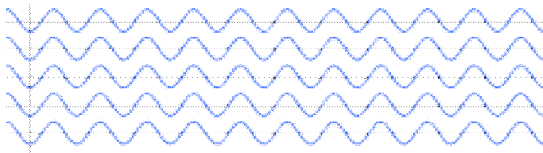


Fig (2.3) Incoherent light waves



Fig(2.4) Coherent light waves

Spatial coherence: It is degree to which a beam of light appears to have originated from a single point in space

Temporal coherence: It is the extent to which all the photons in a light beam are of the same frequency or wavelength.

2.5.4.2 Monochromaticity:

all light consists of waves traveling through space. The color of the light is determined by the length of those waves. Wavelength is the distance over which the wave repeats itself and is represented by Greek letter λ . Monochromaticity is a unique property of laser light, meaning that it consists of light of almost a single wavelength.

2.5.4.3 Directionality:

All conventional light sources emit light in all direction. Light of Laser its output is in the form of an almost parallel beam. Directionality is the characteristic of laser light that causes it to travel in single direction within a narrow cone of divergence.

2.5.4.4.Collimation:

Because of bouncing back between mirrored ends of a laser cavity, those paths which sustain amplification must pass between the mirrors many times and be very nearly perpendicular to the mirrors. As a result, laser beams are very narrow and do not spread very much

2.5.5LASER CLASSIFICATION

Laser can be classified depending on the physical state of the active medium .Each type of laser special feature according to this feature is determined by the application.

2.5.5.1 GAS LASER

Gas laser a large and important family of laser utilizes a gas or gas mixture as the active medium .Excitation usually is achieved by current flow through the gas .Gas lasers may be operated in either CW or pulsed modes. One popular type of gas laser contains a mixture of helium (He) and neon (Ne) gases .The gas mixture is contained at a low pressure within a sealed glass tube called the "plasma tube."The excitation mechanism of the HeNe laser is a direct current discharge through the gas, the current pumps the helium atoms to an excited atomic state. The energy of excited helium atoms is transferred to neon atoms through collisions, and the neon atoms then undergo a transition to a lower energy state that results in lasing. The feedback mechanism consists of a pair of mirrors sealed to the ends of the plasma tube. One of these mirrors, the output coupler, transmits 1-2 a percent of the light to form a continuous (CW) output beam. There are other types of gas laser such as Helium- Cadmium (He-Cd), the molecule gas laser it is Carbon Dioxide (CO₂) and Nitrogen(N₂) .The ion gas laser Argon ion (Ar⁺) and Krypton ion (Kr⁺).The metal vapor laser: Copper vapor (Cu) and Gold vapor (Au).

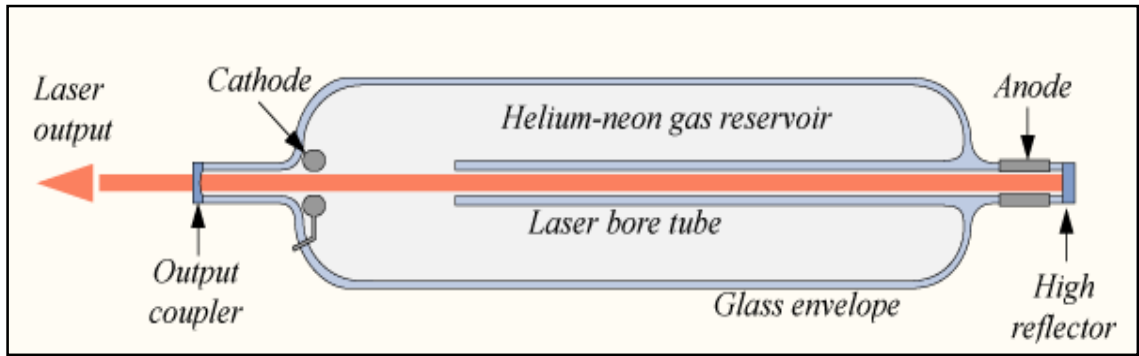


Fig (2.5) He Ne laser

2.5.5.2 LIQUID DYE LASERS

Liquid dye lasers use a solution of a complex dye material as the active medium. The dyes are large organic molecules, with molecular weights of several hundred. The dye material is dissolved in an organic solvent, like methyl alcohol. Thus, the active medium is liquid. Dye lasers are the only types of liquid lasers which have reached a well developed status. One of the most important features that dye lasers offer is tenability, that is, the color of the output beam can be varied by adjusting the internal tuning element and also by changing the type of dye that is used. The monochromatic output of available dye lasers can be tuned over a broad range, from the ultraviolet, to the infrared. Liquid dye lasers that can be tuned to any visible wavelength, and portions of the infrared and ultraviolet, are commercially available in both pulsed and continuous models. Dye lasers are chosen for applications, like spectroscopy, in which tenability is important.

2.5.5.3 SEMICONDUCTOR LASERS

The semiconductor or diode lasers are the smallest of all the known lasers; they have a size of a fraction of a millimeter. The laser consists of a semiconducting crystal, such as gallium arsenide, lead selenide, etc, with parallel faces at the ends to serve as partially reflective mirrors. A semiconductor, as the name implies, is half-way between a conductor

and an insulator (non-metal), so far as its electrical conductivity is concerned. There are two types of semiconductors, viz., n-type and p-type. To understand the functioning of these devices, it is necessary to know the nature of the electronic energy states in a semiconductor. A typical semiconductor has bands of allowed energy levels separated by forbidden energy gap region. In an intrinsic semiconductor, there are just enough electrons present to fill the uppermost occupied energy band (valence band) leaving the next higher band (conduction band) empty. In an n-type semiconductor, a small amount of impurity is added intentionally so that the material is made to have an excess of electrons, which thus becomes negative. On the other hand, by adding a different type of impurity in a p-type semiconductor, the material can be made to have an excess of holes (vacancy of electrons), which thus becomes positive. The semiconductor laser consists of a tiny block (about one square millimeter in area) of gallium arsenide when the p- and n-type layers are formed in an intimate contact, the interface becomes a p-n junction. When direct current is applied across the block, the electrons move across the junction region from the n-type material to the p-type material, having excess of holes. In this process of dropping of the electrons into the holes, recombination takes place leading to the emission of radiation. The photons travelling through the junction region stimulate more electrons during the transition, releasing more photons in the process. The laser action takes place along the line of the junction. Due to the polished ends of the block, the stimulated emission grows enormously and a beam of coherent light is emitted from one of the two ends. With a gallium arsenide laser, a continuous beam of a few milliwatts power is easily obtained. The semi conducting lasers are also called junction lasers or junction diode lasers because they produce laser energy at the junction of two types of impurities in a semiconductor.

They are also called injection lasers because electrons are injected into the junction region. Semiconductor lasers usually have outputs in the infrared wavelength range, although some models that emit in the visible region are available.

2.5.5.4 SOLID STATE LASERS

A solid state laser another important family of lasers, it contains solid crystalline or glass material as an active medium. Ruby and neodymium are two common examples of solid lasers with widespread Industrial applications. Ruby is crystalline aluminum oxide in which some of the aluminum ions in the crystal lattice have replaced by chromium ions. These chromium ions are the active elements in the ruby laser.

2.5.5.5 Nd: YAG Laser

Nd:YAG laser is considered as one of the most commonly used types of laser and it has many applications. It uses a flash light or a diode laser as an optical pump. It emits light at different wavelengths, the main one is in the infrared region (IR) with a wavelength of 1064 nm. Nd:YAG lasers operate in two modes:

a-Continues mode

In the continuous mode the atoms are stimulated by the optical pump and as they release their energy the laser is emitted, but this one is not as powerful as the pulsed one.

b-Pulsed mode (Q-switching mode)

In this mode, an optical switch (Q-switch) is placed in the laser cavity of the Nd:YAG lasers. This switch only opens when the population inversion is maximum in the neodymium ions. When it opens it allows the light to flow in the cavity depopulating the excited laser medium at maximum population inversion. In this Q-switched mode, output powers

of 250 megawatts and pulse durations of 10 to 25 nanoseconds have been achieved. The high-intensity pulses may be efficiently frequency doubled to generate laser light at 532 nm, or higher harmonics at 355 and 266 nm. Nd:YAG absorbs mostly in the bands between 730–760 nm and 790–820 nm. So in order to select a good optical pump, the wave length of the emitted light should be taken into consideration. At low current densities krypton flash lamps have output between 760 and 810 nm, so it works fine more than the ordinary Xenon lamps for pumping Nd:YAG lasers.

The amount of the neodymium dopant in the material varies according to its use. For continuous wave output, the doping is significantly lower than for pulsed lasers. The lightly doped continuous wave rods can be optically distinguished by being less colored, almost white, while higher-doped rods are pink-purplish

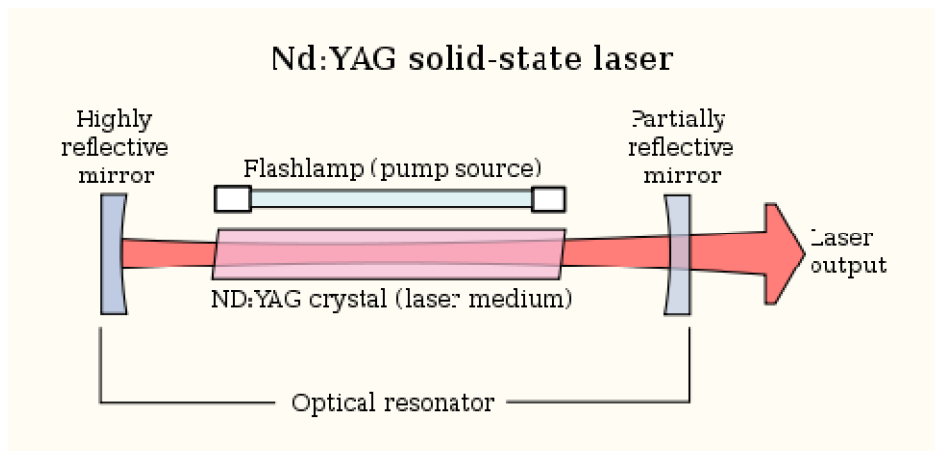


Fig (2.6) show Nd:YAG laser

2.5.6 Pulsed Laser Ablation (PLA)

Pulsed laser ablation (PLA) is a process in which a pulsed laser beam is applied to remove/eject material from a solid surface. There are two kinds of PLA depending on the surrounding medium during the interaction between the laser beam and the material. PLA of materials in the presence of gases or in vacuum has been used to synthesize a wide variety of thin films and this is well known as Pulsed Laser Deposition (PLD) technique. On the other hand, PLA of a powder/solid target which is dispersed /immersed in liquid is now known as Pulsed Laser Ablation in Liquids. Fig (2.7)

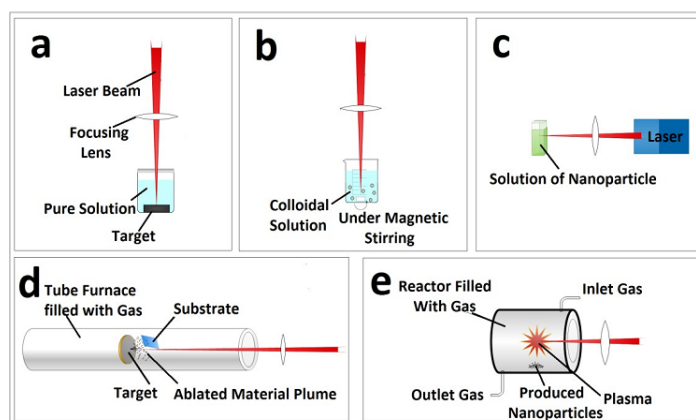


Fig (2.7)PLS systems where a focused beam irradiates: a) a solid target placed in a pure solution; b) a colloidal solution; c) a solution of nanoparticles is irradiated by a focused beam; d) a solid target placed inside a tube furnace with a nearby substrate to collect the material deposition; and e) a reactor filled with a gaseous precursor

2.5.7 Fundamentals of interaction of the laser beam with the matter

The interaction of the laser radiation with matter is the most important issue in the synthesis of nano materials with laser beams. The use of PLS for manufacturing new materials involves the appropriate

selection of the laser's processing parameters with respect to the photo-physical properties of the material on which it is applied. In this section, basic concepts regarding the most common interactions of laser radiation and matter are presented.

2.5.7.1 Excitation Mechanisms of Matter Irradiated by Pulsed Laser

When the laser beam interacts with a material in vacuum, gaseous or liquid medium, the incident light can either be reflected or absorbed. The absorbed energy from the laser beam can react with the matter in a form of either a thermal or/and chemical process. Generally, the mechanisms that can possibly occur as a result of the laser- matter interactions can be categorized into two possible mechanisms. These possible mechanisms as photochemical, photothermal and photophysical, are described below. For interactions between the laser and matter, the following factors should be taken into consideration

Physical state of the material , i.e. solid, liquid or gas.

Type of the material, i.e. conductor, insulator, or semiconductor

Laser beam parameters: excitation wavelength, pulse width ,laser fluence, and beam diameter.

Impurities, defects,and crystal structure of the solid material in two interfaces experiments.

Relaxation times of thermalization and initial excitation processes

2.5.7.2 Photothermal Mechanism

The photothermal mechanism induced by a pulsed laser refers to the thermal activation processes inside the material, where there is a phase change due to an increase in the temperature and enthalpy of the system. The absorbed photon energy induces an excitation within the focused area of the focused pulsed laser. These types of excitations

are known as the photothermal effect, thermal explosion, or pyrolytic effect, and are usually described by the relaxation times. In photothermal processes the laser evaporates the material at higher laser

fluence, which in turn creates heterogeneous nucleation of vapor bubbles leads to normal boiling. In this situation, rapid homogeneous nucleation and expansion of vapor bubbles lead to explosive boiling or phase explosion, which carry off the solid-liquid material fragments. Therefore, the PLS technique can provide significant changes to the irradiated material, opening new chemical reaction pathways and reaction products, and generate novel material microstructures, nanostructures, phases, surface morphologies, and evaporation characteristics.

2.5.7.3 Photochemical Mechanism

The photochemical mechanism term is used for non-thermal reactions induced by photons, which are strong enough to break the bonds between molecules and generate electrons, atoms and ions. The system is described as photochemical or photolytic when the non-thermal processes are the most dominant. Laser irradiation of the matter generates large excitation in the intermediary states, which induce the photo decomposition of the chemical bonds between the molecules of the material.

2.5.7.4 Pulsed Laser Ablation in Liquids Mechanisms

Synthesis of nanomaterials using PLAL technique falls under top-down approach category. In PLAL technique, the production system does not require costly chambers and high vacuum pumps. Also, the preparation of well crystallized NPs using PLAL could easily be attained in one-step procedure without subsequent heat-treatments. In addition, pure NPs could be produced using this technique without the formation of by-

products. Furthermore, the entire product could be collected in solution and the obtained colloidal solution can be easily handled. Moreover in this technique, the size (micrometer/nanometer), composition (pure metals, semiconductors, metal oxides, metal peroxides, alloys, nitrides, carbides, etc.) and morphology (particles, cubes, rods, sheets, tubes, plates, flowers, etc.) of the synthesized materials depend on incident pulsed laser beam characteristics including pulse duration, wavelength, pulse repetition rate, laser fluence and ablation time, in addition to the confinement of the liquid medium. Finally, it makes it possible to use this technique to resize and reshape the synthesized (by PLAL or other methods) colloidal NPs by the secondary ablation which will be revealed later during this study. Two mechanisms are suggested in PLAL to generate nanostructured materials which are summarized in the following sections:

a-Thermal Evaporation Mechanism

When a high intense pulsed laser beam strikes a solid target, most of the beam is absorbed by the medium at a localized spot and this absorption of the beam leads to the creation of a high pressure and temperature plasma (laser-induced plasma) at the solid/ liquid interface. There are two suggested models by Yang et al. and Zeng and coworkers for the interaction between the produced plasma and the liquid environment which in turn leads to synthesize the nanomaterials. Yang et al. proposed that the laser-induced plasma evaporates and excites the confining liquid, converting it to plasma (plasma- induced plasma). The reaction between these two kinds of plasmas was responsible of the production of the nanostructured materials. On the other hand, Zeng and coworkers proposed that the laser-induced plasma expand adiabatically, leading to a quick condensing of the plasma which in turn leads to the fabrication of

clusters. These clusters interact with the liquid medium, resulting in the fabrication of nanostructured material.

b- Explosive Ejection Mechanism

In this mechanism, hot nano droplets are ejected from the target into the surrounding liquid at high speed due to the pulsed laser beam which in turn interacts with the liquid gradually from the surface. The morphology and the chemical composition of the products are governed by the interaction between the ejected nano droplets and the ambient liquid which in turn depends on the medium reactivity and laser parameters. In addition, PLA of a powder material dispersed in a transparent liquid is used to decrease the size of the particles into the nano scale. The synthesized nanoparticles may have the same or different shape, phase and composition depending on the interaction between the ablated particles and the surrounding medium. In this case, two mechanisms are suggested for the ablation of powder targets. The first mechanism is a thermal process in which a pulsed laser beam melts and evaporates the large particles into small species (atoms and molecules) which in turn rearrange themselves into nanostructured particles that have the same or different morphology and structure depending on the reactivity of surrounding medium and laser parameters. The second is known as columbic explosion mechanism in which laser beam ejects electrons from the outer surface of the suspended particles via photoelectron or thermal effect. The electrostatic repulsion between the induced surface charges (positive charges) on the different parts of the particles leads to the explosion of the primary particle into many smaller parts, a process called fragmentation. This leads to synthesis of ultrafine nanoparticles

CHAPTER THREE

METHODOLGYAND CHARACTERIZATION

3.1 The Tools

3.1.1 Nd:YAG laser

Nd:yag laser(Brilliant B) was used operating at 532nm wavelength and maximum pulse energy of 450m J with pulsed width of 5ns and operates at 10 Hz pulse repetition rated



Fig (3.1):Nd-YAG Laser

3.1.2 The Target

The target was used metallic copper (purity 99.99% Advent Research Materials Ltd).fig(3.2)



Fig (3.2) The Target- metallic copper

3.1.3 Other tools

- The magnetic rotater
- The prism and lens

3.2 Experimental Setup for Synthesis of Nanoparticles (NPs)

An intense pulsed laser beam from a Q-switched Nd -YAG laser (Brilliant B) operating at 532 nm wavelength using second harmonic generator was used as an ablation source. This laser can deliver maximum pulse energy of 450 mJ with a pulse width of 5 ns and operates at a 10 Hz pulse repetition rate. With an appropriate turning prism and lens, the laser beam was routed and focused on the sample target. In order to avoid any crater on the target surface due to the high intense laser beam, the target was rotated using a magnetic rotator whose speed was controlled by a stepping motor. The target was kept in the presence of an appropriate liquid medium. The height of the liquid level in the beaker was maintained approximately 2-4 mm above the surface of the target in order to avoid the laser beam travelling a longer path length through the liquid and hence to minimize the absorption loss. The schematic diagram of the ablation

system applied for the synthesis is depicted in Fig. 3-3. In order to get homogeneous solution, a speed magnetic the experiment. Fig. 3-4 shows a photograph of the focusing arrangement of the setup applied. In this work.

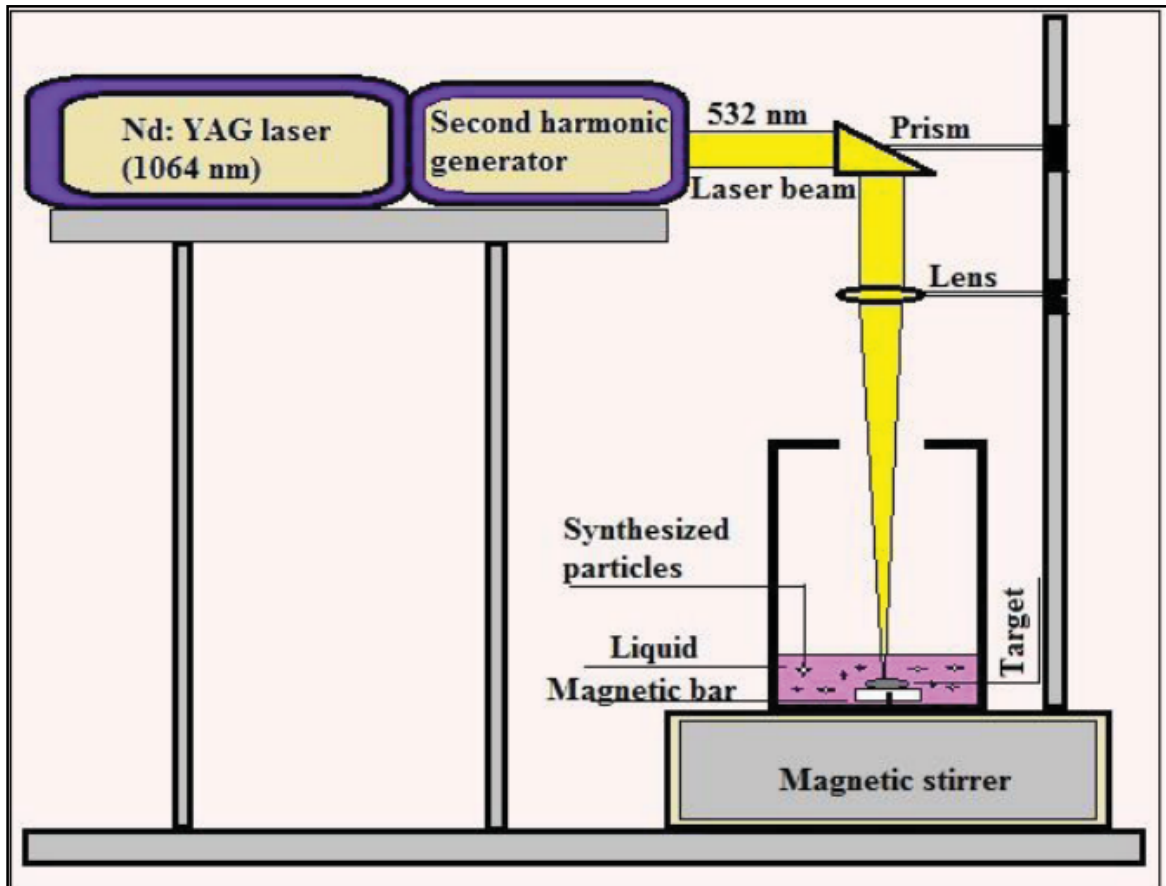


Fig 3-3 Schematic diagram of the focusing arrangement of the setup for synthesis of nanostructured semiconductors from solid target using PLAL technique

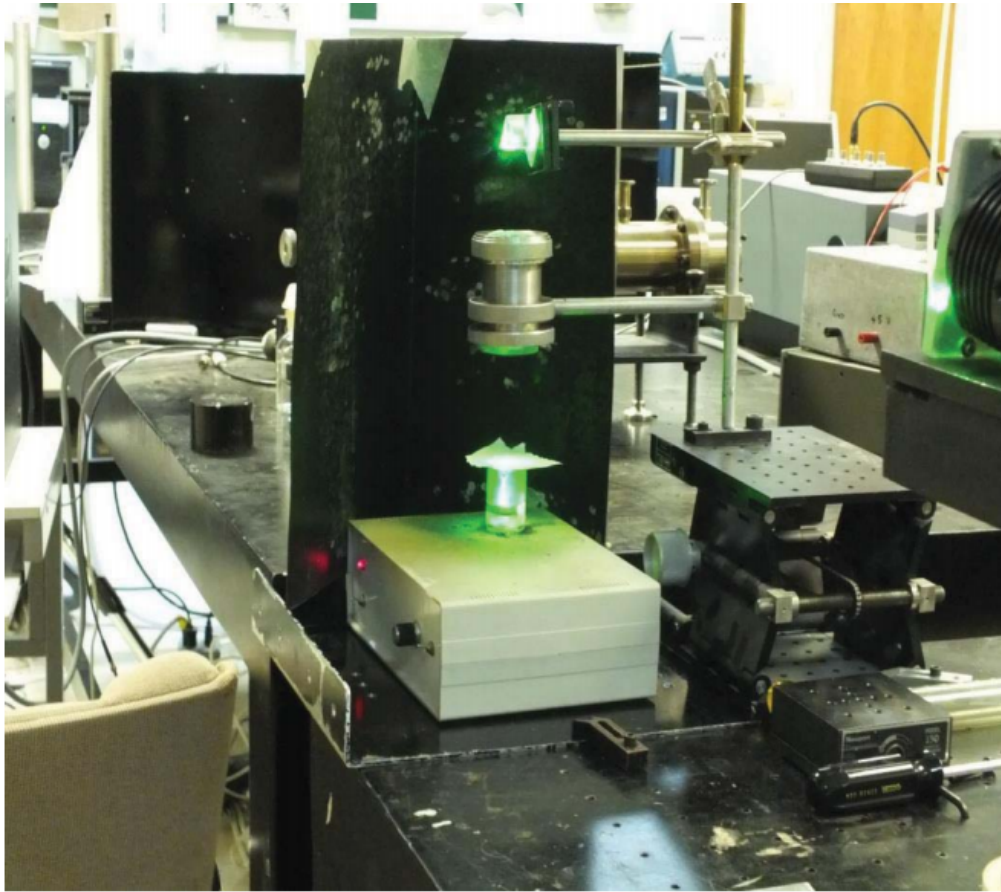


Fig 3-4 Photograph of PLAL setup developed at Laser Laboratory of KFUPM.

It is relevant to mention the problems that we faced at the beginning of this work related with experimental work which could affect the ablation efficiency. These steps are mentioned briefly in the following points:

1. Adjusting the diameter of the magnetic rotator:

Fig. 3-5 shows (a) a glass cell, (b) a magnetic rotator, (c) a target and (d) the final design (a-c together) that was used in the experiment. The diameter of the magnetic rotator (2.5 cm) should be very close to the diameter of the glass cell (2.8 cm) to minimize the vibrations on the liquid surface which in turn decrease the reflectance of laser beam from the liquid surface and increase the ablation efficiency.

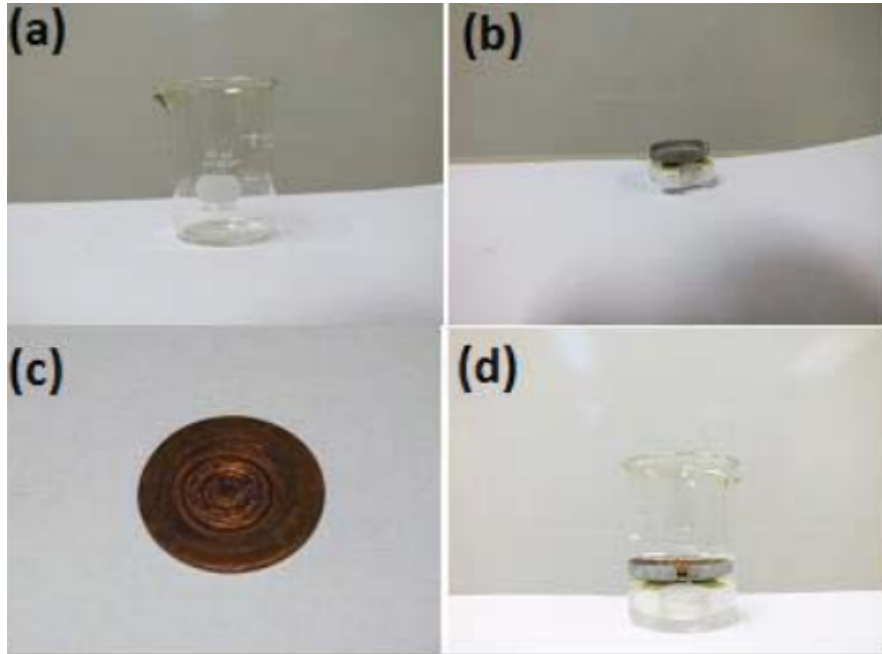


Fig 3-5 Photographs of the essential parts in PLAL: a-glass cell, b-magnetic rotator, e-target d- (a-c) all parts together.

2. Adjusting liquid level above the target surface:

The ablation efficiency could be affected by the liquid level above the target surface. To study this effect, the liquid level was varied from 1 to 10 mm in height from the target surface, and it was found that the typical liquid level should be in the range 2-4 mm as shown in Fig. 3-4. If it is less than this range, the ablated material could fly in air due to the incomplete confinement for the ablated material by the liquid. On the other hand, if it is more than this range, the laser beam could travel a longer path length through the liquid and this means more laser energy absorption by the liquid. In addition, there is a probability that liquid can act as lens and could diverge the laser beam and thus decreasing the ablation efficiency.

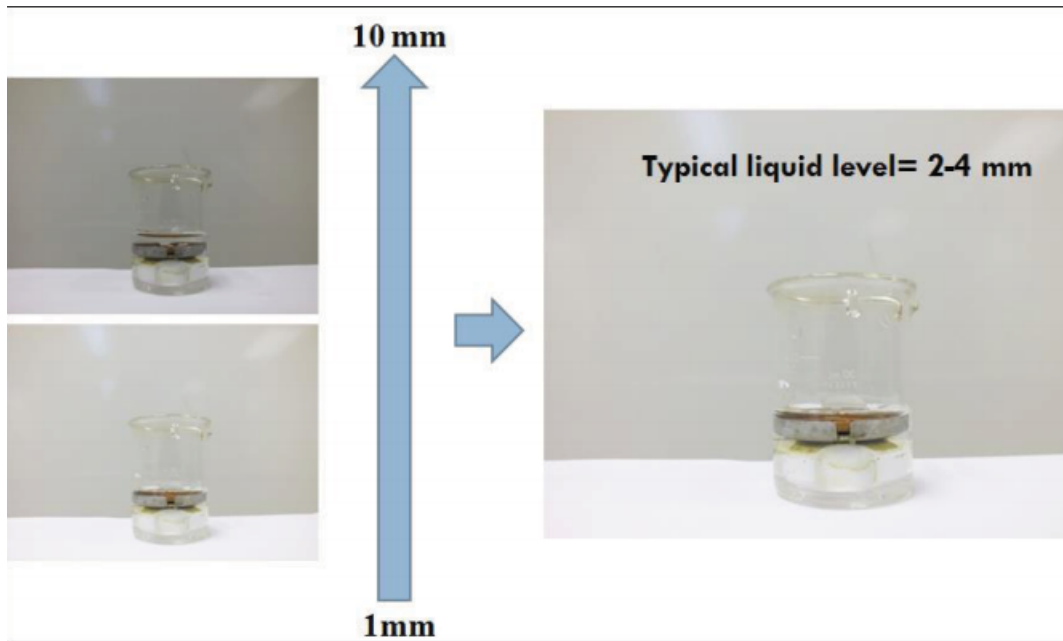


Fig 3-6 Photograph of the glass cell and the magnetic rotator with different volumes of liquid.

3. The height of the magnetic rotator:

Two different designs of magnetic holders were used in the experiment as Shown in Fig. 3-7 -a and -b. Design (b) gives better results, because it allows to use 7 ml of liquid while one can use just 3 ml in design (a) when typical liquid level above target in both of them is 2 mm. The lesser amount of liquid in design (a) means higher concentration of ablated material for the same period of time and this means higher absorption, reflection and lower ablation efficiency.

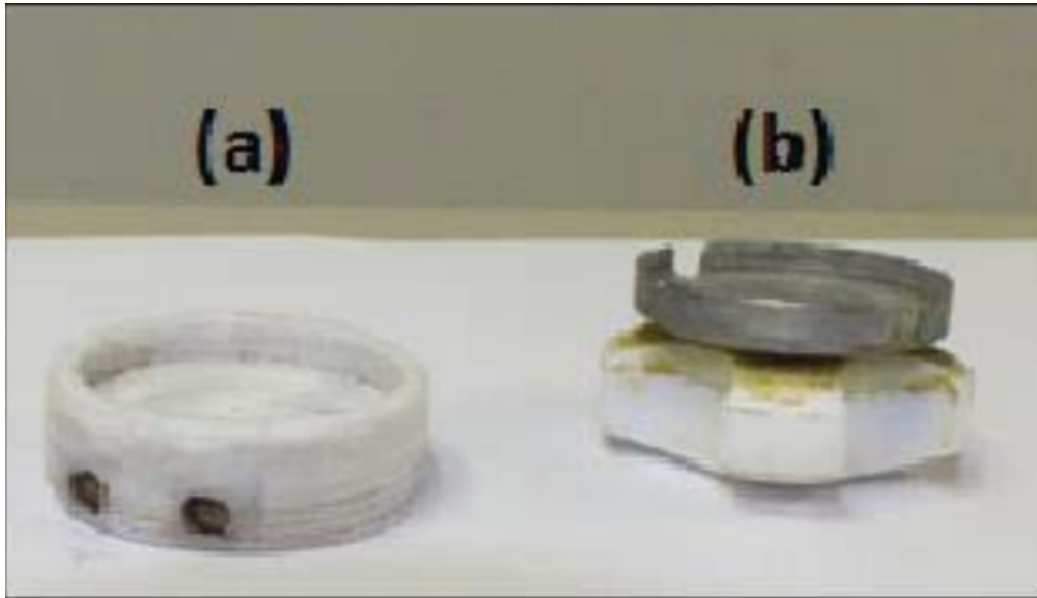


Fig 3-7 photographs of different designs of magnetic rotator

3.3 Characterization Techniques for Synthesized Nanoparticles

After 15 minutes of ablation, the produced colored colloidal suspension of nanostructured Semiconductors were collected and dried in an oven at low temperature. The structure, Composition and the morphology of the product material were investigated using X-ray Diffraction spectroscopy (XRD), Energy Dispersive X-ray Spectroscopy (EDS), Field Emission Scanning Electron Microscopy (FE-SEM) and Transmission Electron Microscopy (TEM). The optical properties of nanostructured semiconductors were investigated using spectrofluorometer (PL) and UV-Vis spectrophotometer.

3.3.1 X-ray Diffraction (XRD)

The XRD was carried out using X-ray diffractometer (Shimadzu XRD Model 6000) using Cu-K α radiation, operated at 40kV and 30mA. This

system is located in the Surface Science Laboratory, Physics Department, King Fahd University of petroleum and minerals (KFUPM) and depicted in Fig.(3.8)



Fig 3-8 Photograph of the X-ray diffractometer used in this study.

3.3.2 Field Emission Scanning Electron Microscopy (FE-SEM)

For surface morphology studies the Field Emission Scanning Electron Microscopy (FESEM, TESCAN Ultra-High Resolution) was used by operating at 20kV with different magnification powers. This Scanning electron microscope is also equipped with an X-ray energy dispersive spectroscopy(EDS) detector as shown in Fig. 3-9. This system is located in Center of Excellence in Nanotechnology (CENT), KFUPM.



Fig 3-9 Photograph of FE-SEM and EDS systems used in this work.

3.3.3 UV-Vis Spectrophotometer for Band Gap Measurements

The UV-Vis absorption spectrum was obtained with the spectrophotometer (Jasco 670). This system is located in Laser Research group, Physics Department, KFUPM and depicted in Fig(3.10).



Fig 3-10 Photograph of UV-Vis spectrophotometer used in this work

3.3.4 Spectrofluorometer for Photoluminescence Study

The photoluminescence data were taken using Shimadzu Spectrofluorometer with 1200 grooves/mm, and with a suitable excitation wavelength. This system is located in the Laser Research group, CENT, KFUPM and depicted in Fig(3.11).

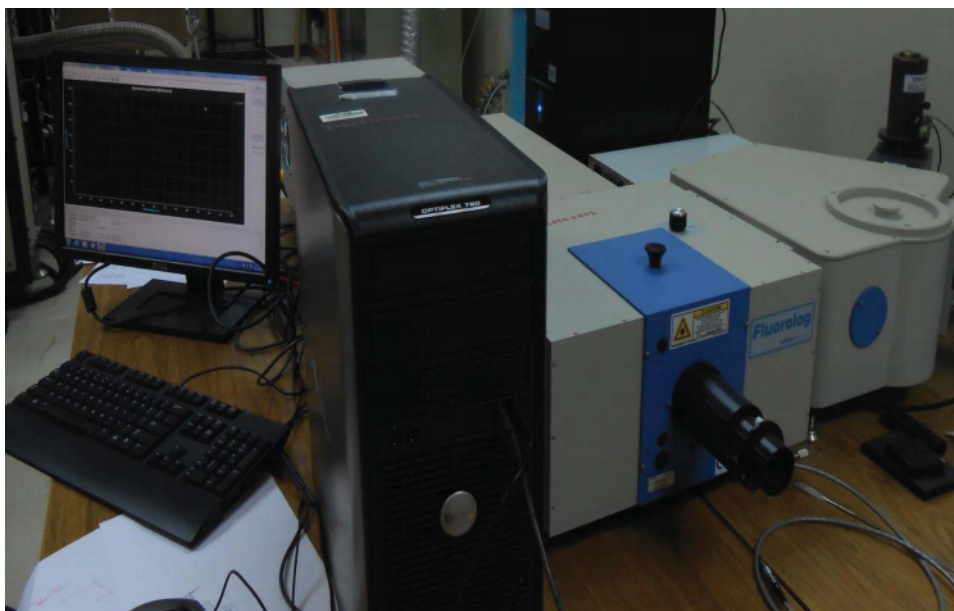


Fig 3-11 Photograph of Spectrofluorometer used in this work.

CHAPTER FOUR

RESULTS AND DISCUSSIONS

In this chapter, results and discussion regarding the synthesis of nanostructured semiconductors (copper oxides) using PLAL technique are presented. The composition, morphology and optical properties of the synthesized nanoparticles are also discussed.

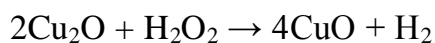
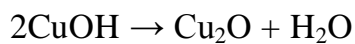
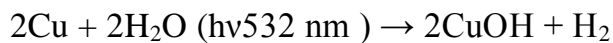
4.1 Synthesis of Copper Oxides NPs

In this section, the synthesis of copper oxides NPs using PLAL technique is discussed. The effects of oxidizing medium and temperature on the composition, morphology and optical properties of the synthesized copper oxide NPs are presented in details in the following two subsections.

4.1.1 Effects of Oxidizing Medium

In this section, the effect of oxidizing media (different concentration of H_2O_2 mixed with DW) on the composition, morphology and optical properties of the synthesized nanoparticles is described. The experimental setup depicted in Fig. 3-3 was employed for this purpose. The target used was 1mm thick metallic copper and it was fixed on the magnetic rotator which was immersed in the liquid medium in the glass cell. Typical energy density and the liquid level above the target surface were $3 J/cm^2$ and 2 mm respectively. In this study, we kept all the experimental parameters the same except the concentrations of H_2O_2 in the DW. Different concentrations of hydrogen peroxide (1, 3 and 5% by volume) were added in the DW during the experiment. After 15 minutes of ablation, the synthesized colored colloidal suspension was collected and

dried at a temperature of 40 °C for 3 hours. The products obtained from PLAL process were characterized with the analytical tools such as, XRD, EDS, TEM, UV-VIS absorption. The results indicated that the higher concentration of H₂O₂ favors not only the production of Cu/CuO but also reshape the copper oxide nanostructures. As it is evident from Fig. 4-1, the suspension of synthesized nanomaterial in the liquid medium show different colors, the darkest one on the left side is the synthesized nanomaterial made without the presence of H₂O₂ in liquid medium. This dark color is due to the presence of predominant copper and Cu₂O in the product material and as we use higher concentration of H₂O₂ in liquid medium, the color of the suspension of the synthesized nanomaterial gets lighter, indicating the presence of less copper and more CuO, which will be more evident from the subsequent discussions below. The possible chemical reactions between the removed copper NPs due to the ablation and the liquid medium (H₂O/H₂O₂) are as follows:



With the increased concentration of H₂O₂, there could be a significant increase in the conversion of Cu₂O into CuO as depicted in the following chemical reaction.



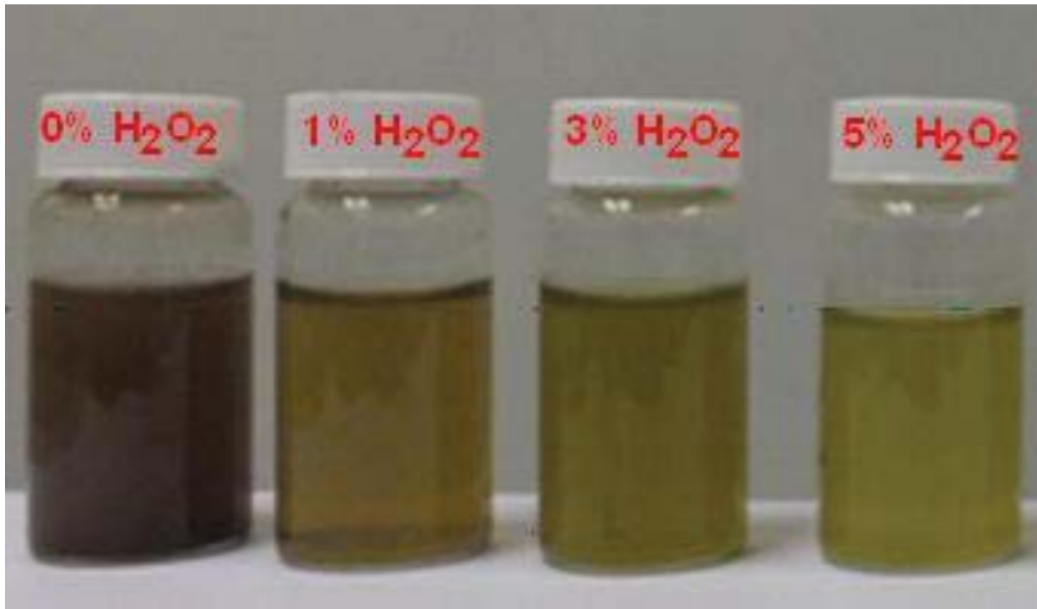


Fig 4-1. The appearance and color of the synthesized nanomaterial samples by varying the concentrations of H₂O₂ in the DW as indicated in the figure.

4.1.1.1 Structure and Morphology of Synthesized Material

EDS spectra for a selected 16 μm² on the surface of the prepared samples are presented along with the quantifications annotated in the inset in Fig. 4-2, 4-3, 4-4 and 4-5 respectively.

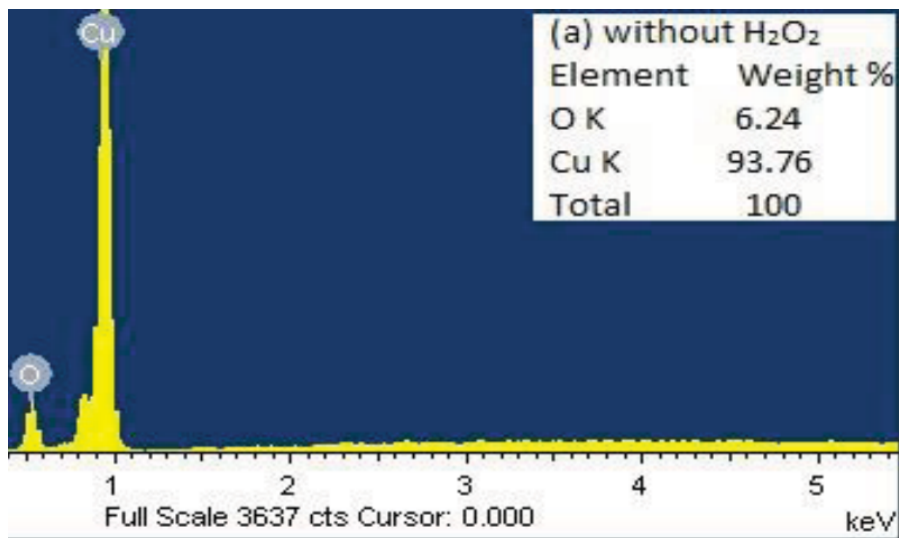


Fig 4-2 EDS spectrum of the synthesized nanomaterial in 0 % of H₂O₂ in the DW as indicated on the figure.

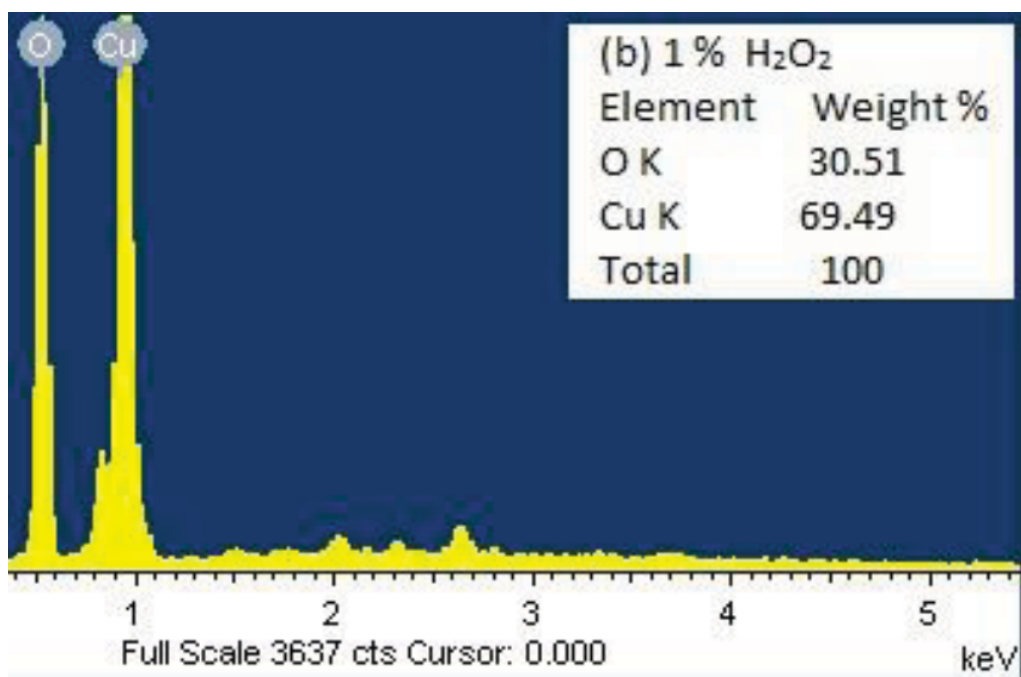


Fig 4-3 EDS spectrum of the synthesized nanomaterial in 1 % of H₂O₂ in the DI water as indicated on the figure.

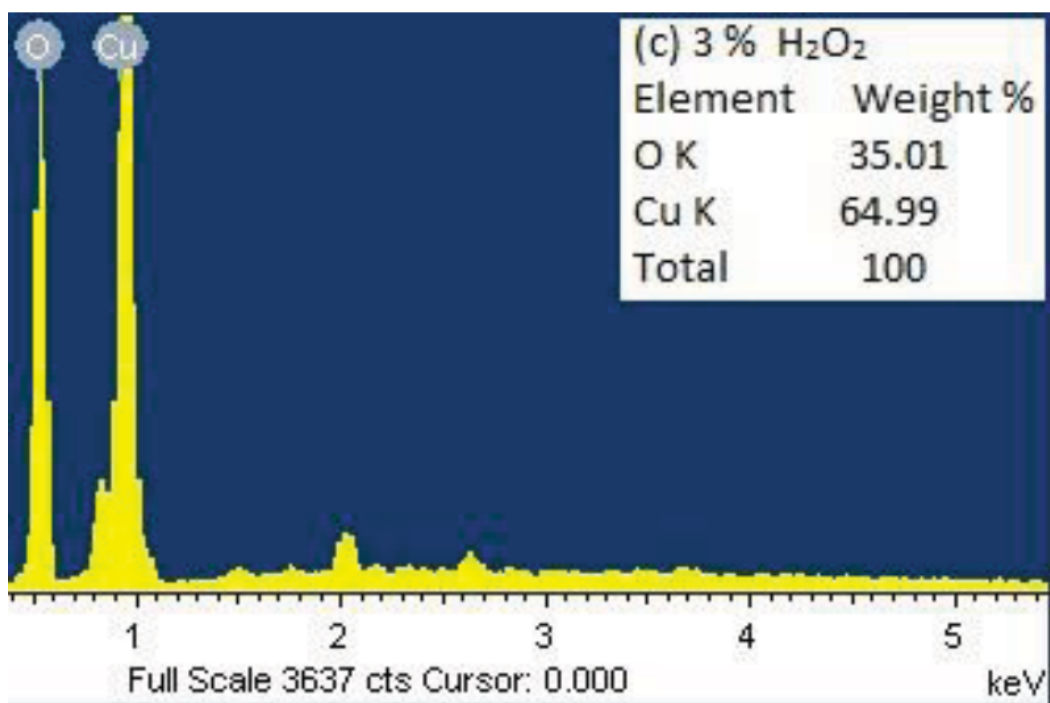


Fig 4-4 EDS spectrum of the synthesized nanomaterial in 3 % of H₂O₂ in the DW as indicated on the figure.

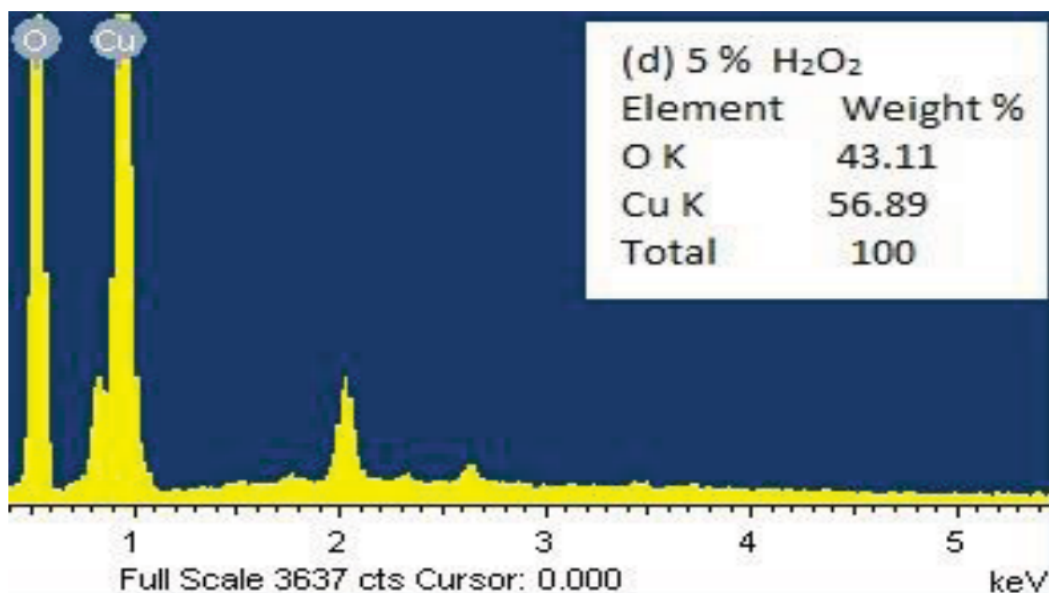


Fig 4-5 EDS spectrum of the synthesized nanomaterial in 5 % of H₂O₂ in the DW as indicated on the figure.

The presence of copper and oxygen in the EDS confirms the presence of copper oxide and also the results showed the increase of the relative mass percentage of oxygen to copper with the increased concentration of H₂O₂ as clear from Fig. 4-2 through 4-5. X-ray diffraction patterns of the synthesized nanomaterial are shown in Fig. 4-6, -7, -8 and -9.

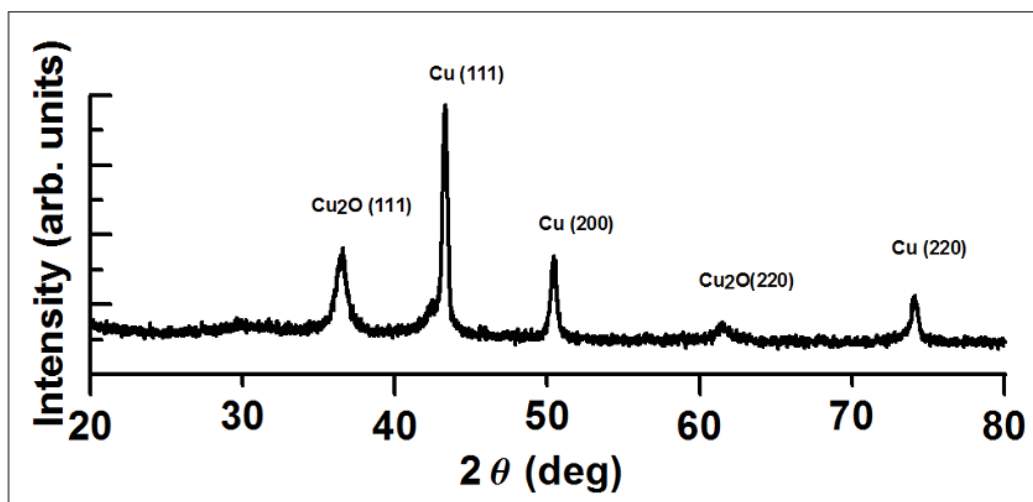


Fig 4-6 X-ray diffraction of the synthesized nanomaterial in 0 % of H₂O₂ in the DW.

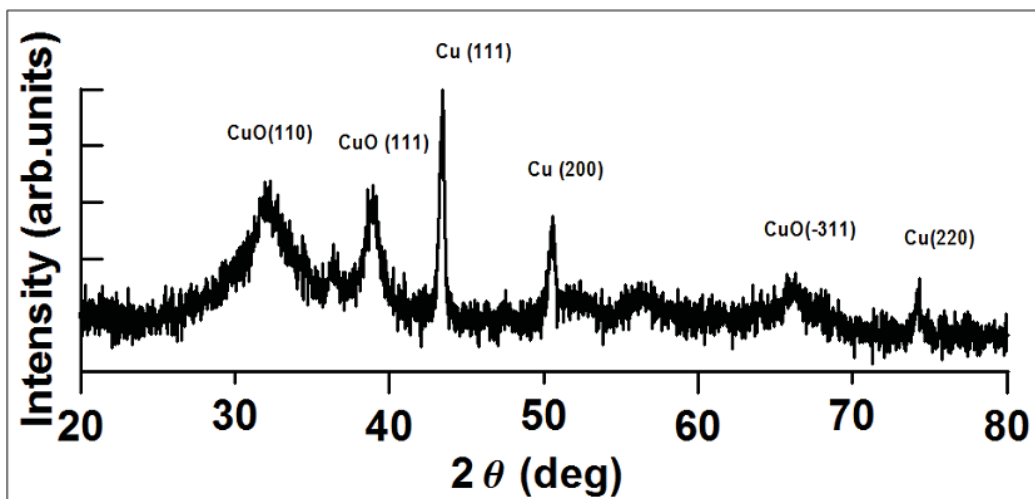


Fig 4-7 X-ray diffraction of the synthesized nanomaterial in 1 % of H_2O_2 in the DW.

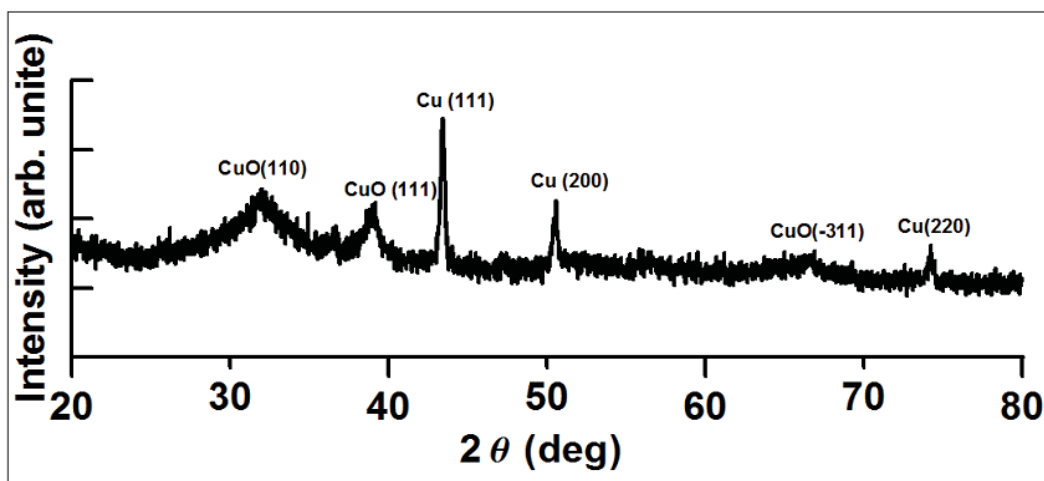


Fig 4-8 X-ray diffraction of the synthesized nanomaterial in 3 % of H_2O_2 in the DW.

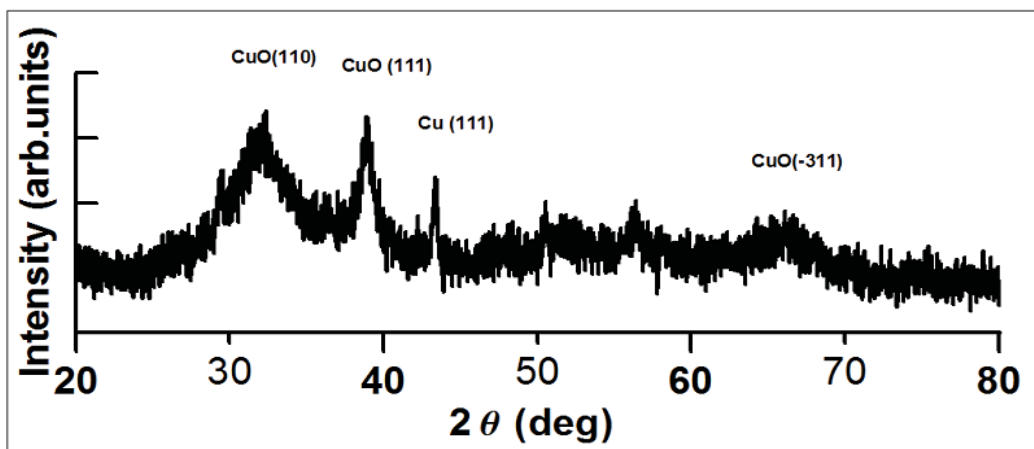


Fig 4-9 X-ray diffraction of the synthesized nanomaterial in 5 % of H₂O₂ in the DW.

In the absence of H₂O₂ in DW, the two phases present in the synthesized material are Cu and Cu₂O as shown in Fig. 4-6 and as 1% of H₂O₂ is added to the liquid medium, the Cu₂O in the product material disappears and CuO appears and its level in the product material increases with the increase of H₂O₂ from 1% to 5% (Fig. 4-7, 4-8 and 4-9) and this result is understandable from the increased oxygen in the liquid medium. The XRD results substantiate the results of EDS. In addition to this, it is quite clear from Fig. 4-7, 4-8 and 4-9 that the FWHM of copper diffraction peaks is smaller than that of cupric oxide ones, indicating that the mean crystal size of the copper grains is higher than that of cupric oxide. In addition to the change of phase composition of the product material with increased H₂O₂ concentration, there is a change of the shape of the nanostructure observed with the increased H₂O₂ concentration. It is clear from the TEM image in Fig 4-10 with no H₂O₂ present, the product material show spherical shape with an average size less than 10 nm, whereas the synthesized nanomaterial with 5% H₂O₂ concentration in DW (Fig. 4-11) shows rod-like nanostructure. In addition, the crystallization of the synthesized nanomaterial in 0% of H₂O₂ is much

better than that in 5% H_2O_2 which is in a good agreement with XRD patterns.



Fig 4-10 TEM image of the synthesized nanomaterial in 0% of H_2O_2 in the DW.

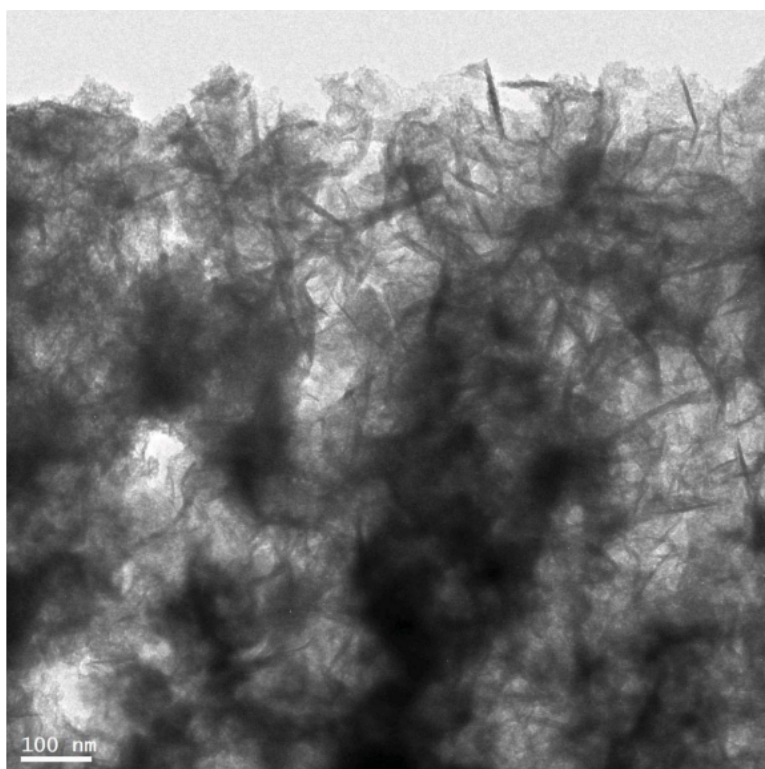


Fig 4-11 TEM image of the synthesized nanomaterial in 5% of H_2O_2 in the DW.

4.1.1.2 Optical Characterization of the synthesized Material

Optical characterization such as absorption was also carried out on the synthesized nanomaterials at room temperature. For all the absorption spectra depicted in Fig. 4-12, 4-13, 4-14 and 4-15, the incident laser beam parameters were kept constant except that the concentration of H_2O_2 present in the liquid medium. Fig. 4-12 for 0% H_2O_2 in DW, Fig. 4-13 for 1% H_2O_2 in DW, Fig. 4-14 for 3% H_2O_2 in DW, Fig. 4-15 for 5% H_2O_2 in DW.

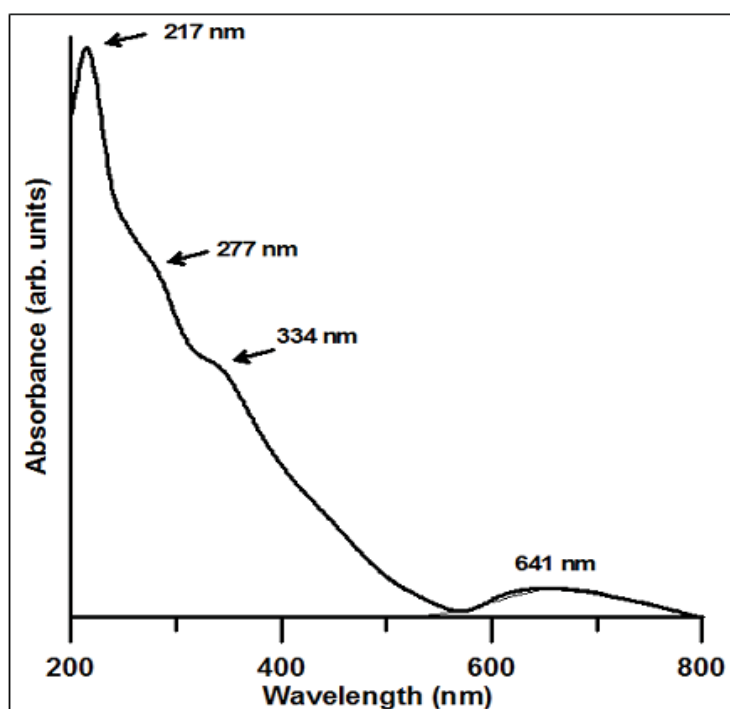


Fig 4-12. Absorption spectrum of synthesized nanomaterial in 0 % of H_2O_2 in the DW.

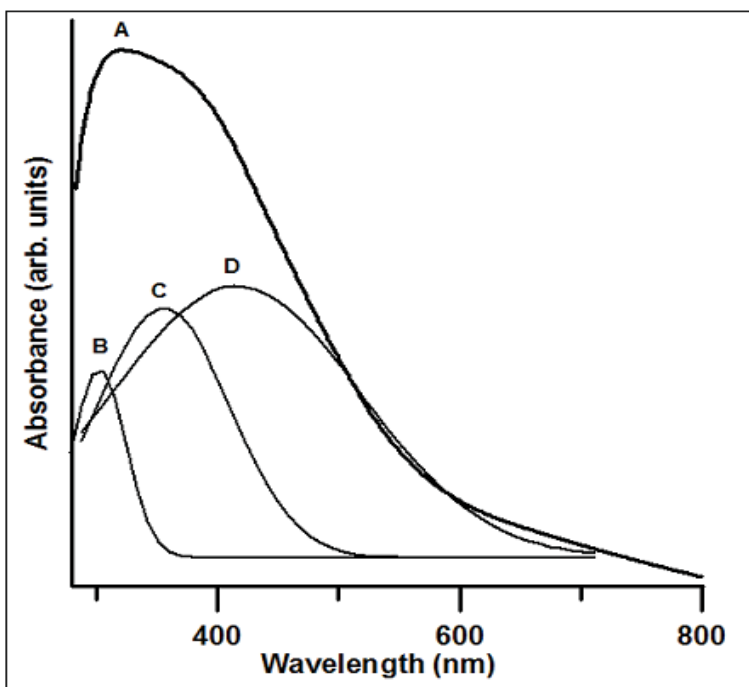


Fig 4-13 Absorption spectrum (A) of synthesized nanomaterial in 1 % of H_2O_2 in the DI water. The Gaussian Peak fit is shown in (B), (C) and (D).

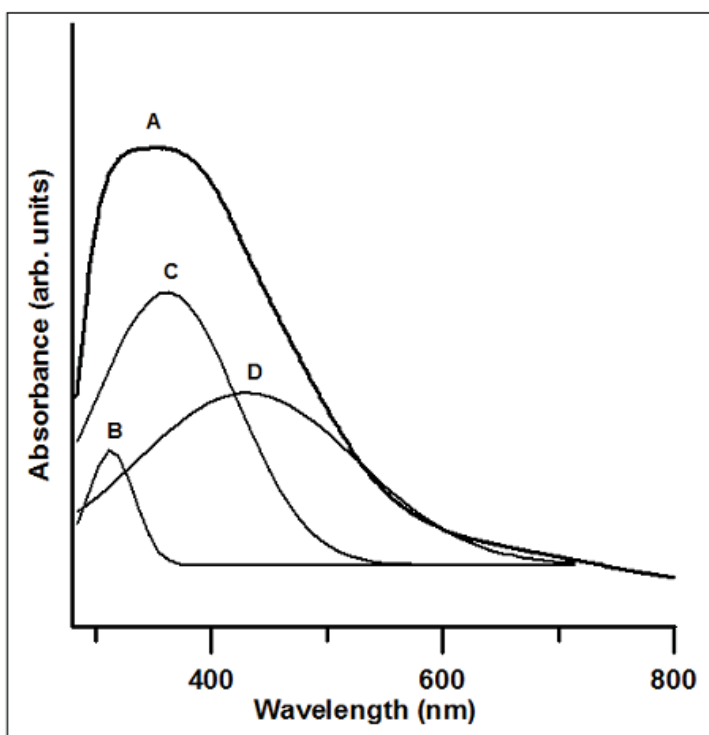


Fig 4-14 Absorption spectrum (A) of synthesized nanomaterial in 3 % of H_2O_2 in the DI water. The Gaussian Peak fit is shown in (B), (C) and (D).

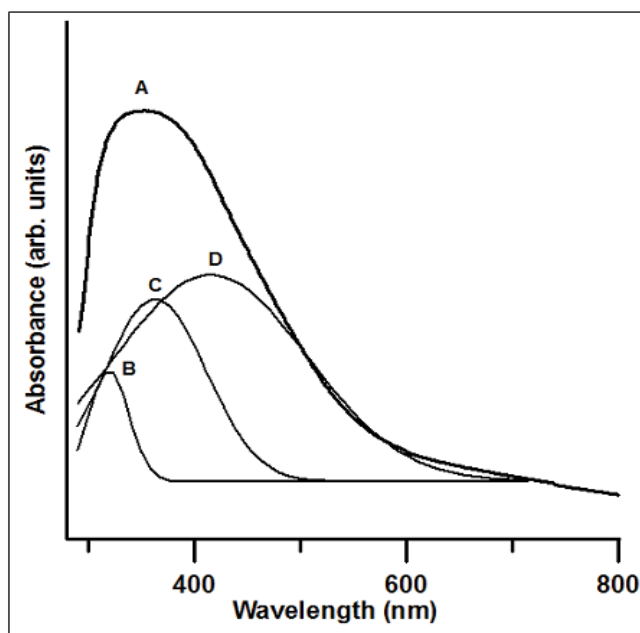


Fig 4-15 Absorption spectrum (A) of synthesized nanomaterial in 5 % of H₂O₂ in the DW. The Guassian Peak fit is shown in (B), (C) and (D).

In the absence of H₂O₂ in the liquid medium (Fig4-12), the product material show four peaks of which the most intense is at 217 nm due to the inter-band transition of copper electrons close to Fermi levels, the broad peak at 641 nm is due to surface Plasmon resonance of Cu and the absorption peaks at 334 nm 277 nm are due to the Brillouin transitions of cuprous oxide. With the addition of H₂O₂ in DW, the absorption spectra (A) of the product material as indicated in Fig. 4-13, 4-14 and 4-15 are broadened indicating the presence of multiple peaks. So we carried out Guassian curve fitting on these broad peaks and found three component peaks (peak B, peak C and peak D) in the absorption spectra. Further increase of concentration of H₂O₂ in DW does not make any substantial change in the characteristics of the component peaks except a minor change in their relative intensities. As the structure and the shape of the synthesized nanomaterial change with the addition of H₂O₂, the plasmonic resonance peak of Cu at 641 nm is absent, which supports our

earlier results. Peak B and C are respectively at 313 nm and 359 nm. The peak at 313 is due to the shape induced charge transfer between 2p oxygen orbital and 4s bands of Cu^{2+} ions and the peak at 359 nm is due to $\text{O}^{2-} \rightarrow \text{Cu}^{2+}$ charge transfer. The origin of peak D needs to be investigated further.

The band gap energy of the semiconductor material can be estimated using Tauc equation (Lee, M.T et al 2009)

$$\alpha E = A(E - E_g)^n \quad (1)$$

Where (α) is the absorption coefficient, (E) is the photon energy, (A) is a constant and n takes the value $\frac{1}{2}$ and 2 respectively for allowed direct and allowed indirect transitions.

$$\alpha E = A(E - E_g)^{\frac{1}{2}} \quad (2)$$

From the absorption data, Tauc plots ($(\alpha E)^2 VSE$) are drawn to determine the band gap energies of the product materials synthesized with varying concentration of H_2O_2 in DW and are shown in Fig. 4-16 for 0% H_2O_2 in DW, Fig. 4-17 for 1% H_2O_2 in DW, Fig. 4-18 for 3% H_2O_2 in DW, Fig. 4-19 for 5% H_2O_2 in DW.

The Tauc plot shows a linear nature over a wide range of photon energy for $n=1/2$ (equation 2) for the ablated material, indicating that the synthesized material is of direct band gap semiconductor.

As it is obvious from the Tauc plots that the band gap energy drastically red shifted from 3.3 eV (376 nm) in the case of zero percent of H_2O_2 in DW (favoring Cu/Cu₂O) to approximately 2.5 eV (496 nm) with the addition of H_2O_2 in DW (favoring Cu/CuO). The minor variation in the band gap energies with increased concentrations of H_2O_2 in DW can be

considered as an experimental variation. As transition metal oxides in general, and copper oxide in particular are good photocatalysts, the red shift brought about in copper oxide by the addition of H_2O_2 in the liquid medium is quite advantageous for any photocatalytic applications. H_2O_2 in the liquid medium shifted the band gap energy to 496 nm, which is active in the visible region of the solar spectrum and hence this material might be suitable as an effective photocatalyst for harnessing the solar radiation.

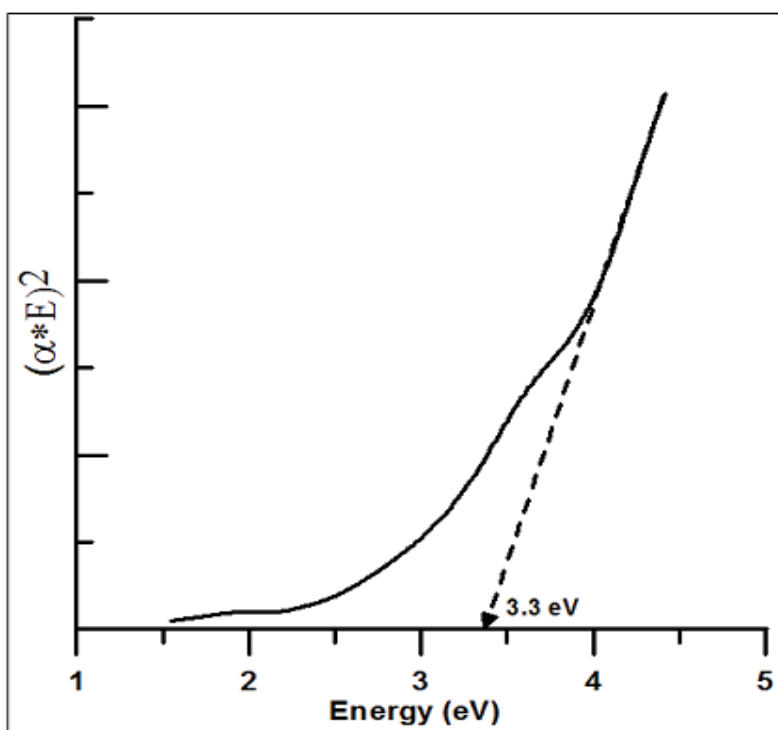


Fig 4-16 Tauc plot of the synthesized nanomaterial in 0 % of H_2O_2 in the DW.

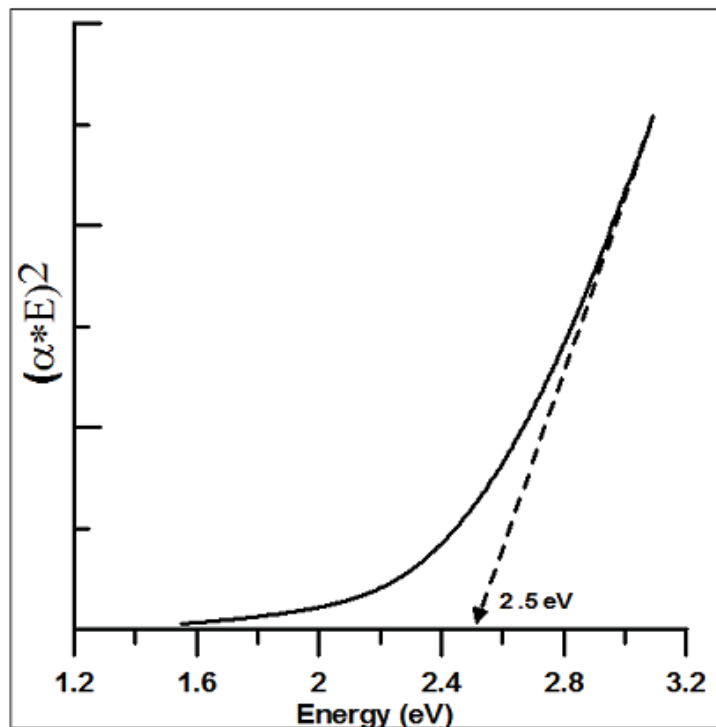


Fig 4-17 Tauc plot of the synthesized nanomaterial in 1 % of H₂O₂ in the DW.

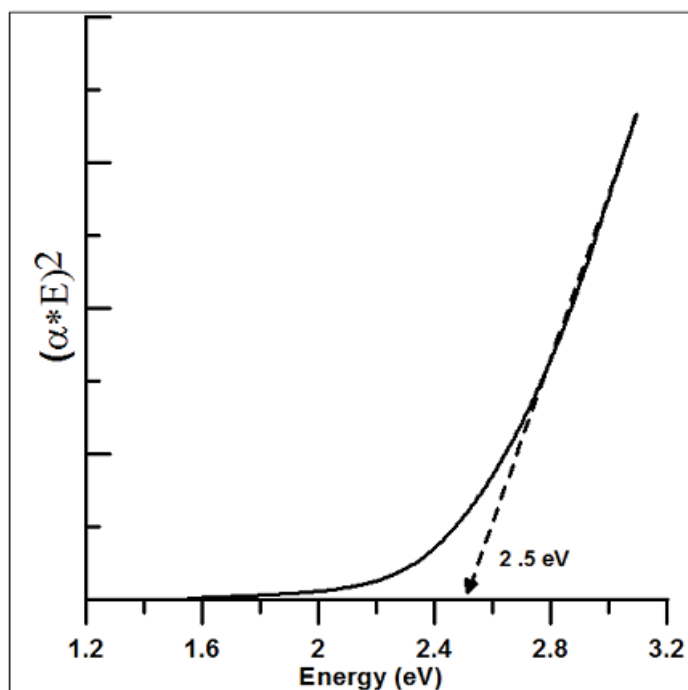


Fig 4-18 Tauc plot of the synthesized nanomaterial in 3 % of H₂O₂ in the DW.

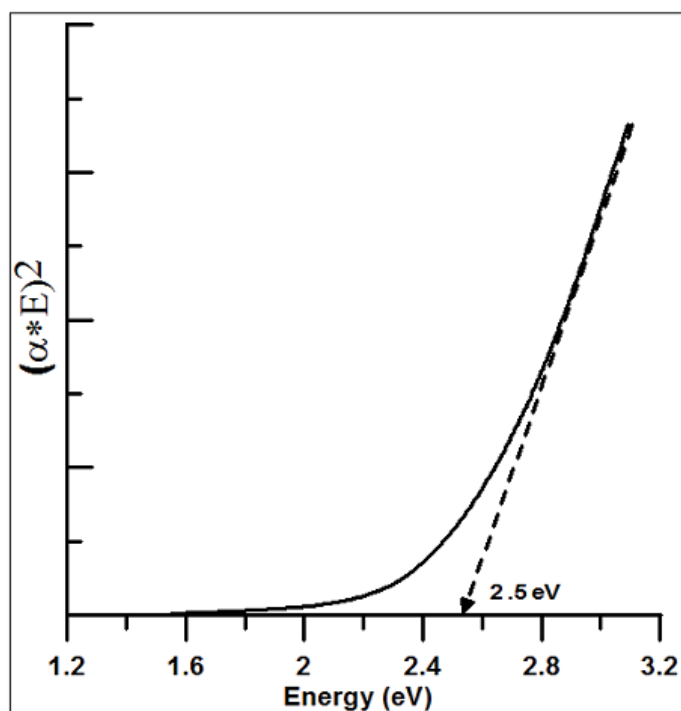


Fig 4-19 Tauc plot of the synthesized nanomaterial in 5 % of H₂O₂ in the DW.

4.1.2 Effects of Annealing Temperature

In this section, the effect of annealing temperature on nanostructured pure copper (Cu) and cuprous oxide (Cu₂O) synthesized using PLAL technique in DI water will be discussed. The same experimental setup and parameters mentioned in section 4.1 were used for this purpose. The ablated material in the DW was filtered out and annealed in air at three different temperatures (300 °C, 600 °C, and 900 °C). In the initial unannealed colloidal suspension, Cu and Cu₂O NPs were obtained and identified as discussed in section 4.1.1. Further we noticed the product (Cu/Cu₂O) was converted predominantly into CuO at annealing temperature of 300 °C for 3 hours. As the annealing temperature was raised from 300 to 900 °C, the grain size of CuO increased from 9 to 26 nm. The structure and the morphology of the prepared samples were investigated using X-ray diffraction and transmission electron

microscopy and UV-Vis absorption spectrometry studies revealed that the band gap and other optical properties of nanostructured CuO were changed due to post annealing.

4.1.2.1 Structure and Morphology of unannealed/annealed Copper oxides NPs

XRD spectra depicted in Fig. 4-20, 4-21, 4-22 and 4-23 show the presence of copper (Cu), cuprous oxide (Cu_2O) and cupric Oxide (CuO) synthesized using pulsed laser ablation.

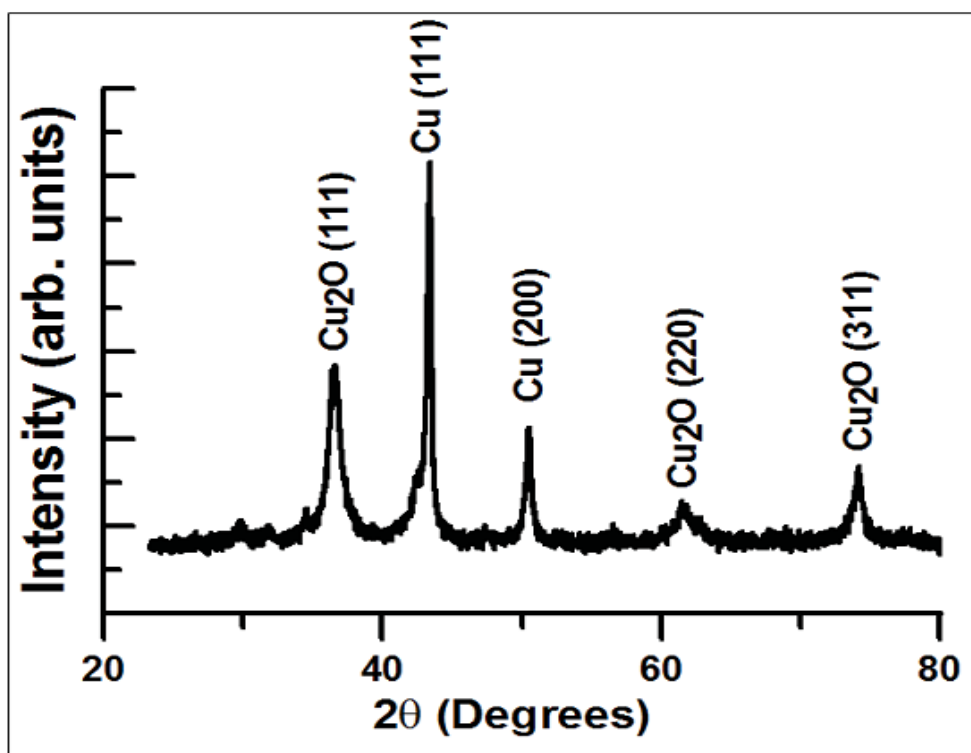


Fig 4-20 X-ray diffraction of Cu/Cu₂O prepared by pulsed laser ablation in DW.

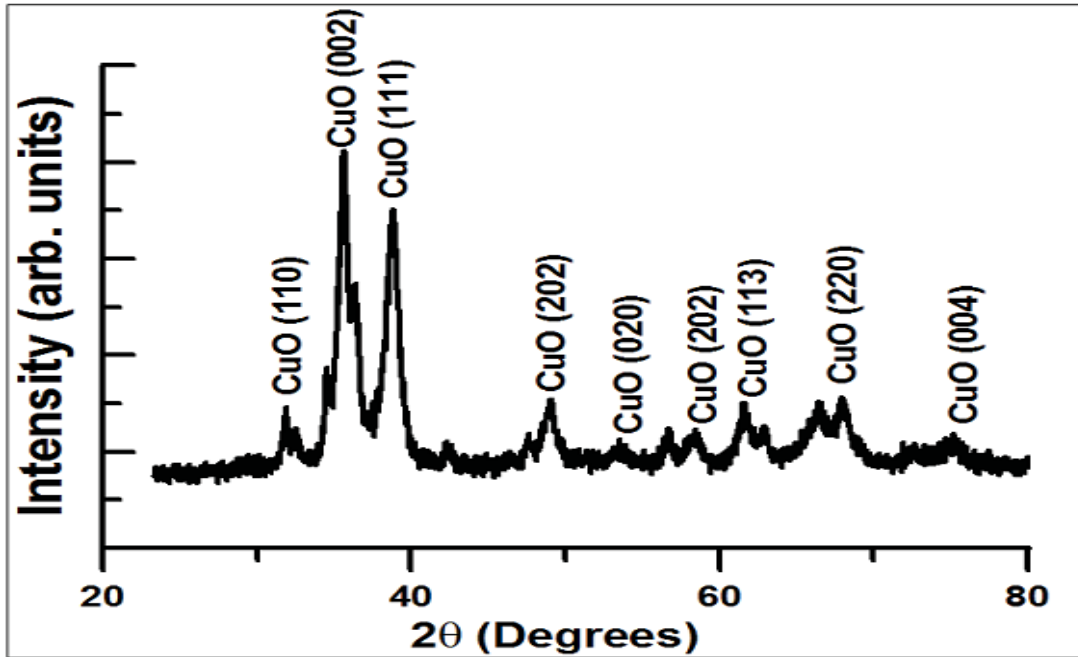


Fig 4-21 XRD patterns of CuO prepared by annealing Cu/Cu₂O at 300 °C for three hours.

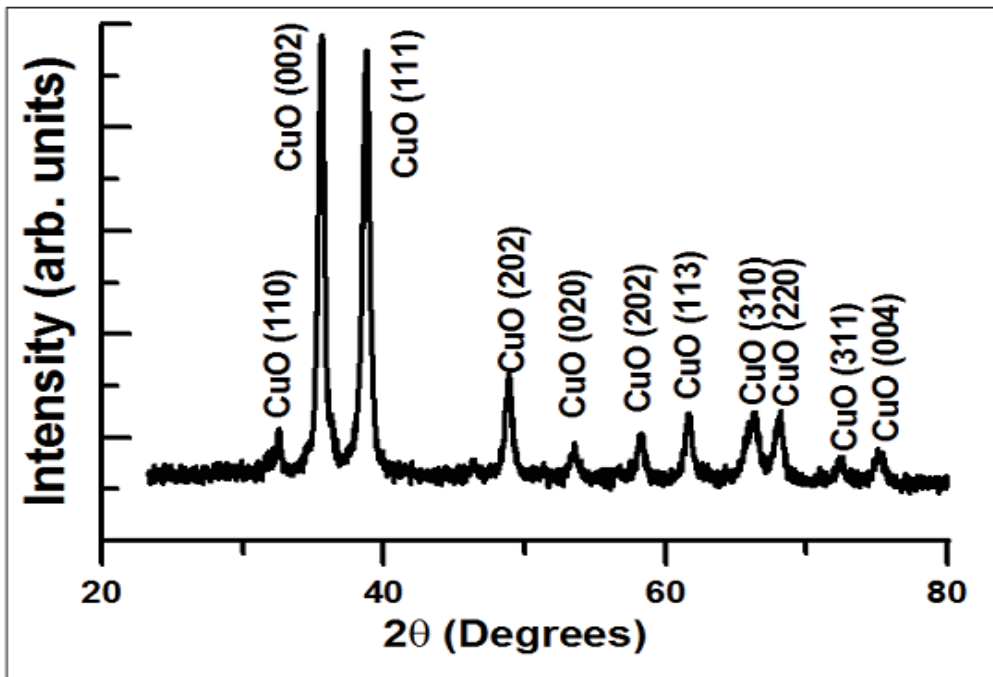


Figure 4-22 XRD patterns of CuO prepared by annealing Cu/Cu₂O at 600 °C for three hours.

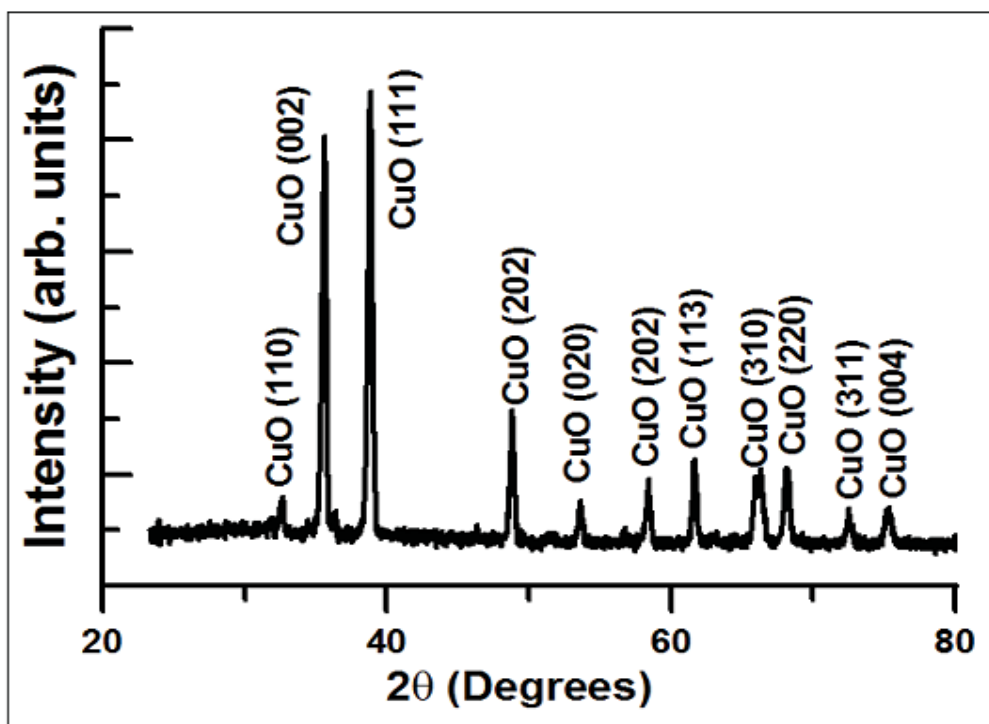


Fig 4-23 XRD patterns of CuO prepared by annealing Cu/Cu₂O at 900 °C for three hours.

As it is clear from Fig. 4-20, the XRD pattern for the synthesized material without subjecting to any annealing, shows the presence of copper (Cu) and cuprous oxide (Cu₂O), and as we anneal the material, a further oxidation brings about cupric oxide (CuO) and gradually depriving the presence of copper (Cu) and cuprous oxide (Cu₂O) as the annealing temperature is raised from 300 °C to 900 °C. In addition to this, the produced CuO became more crystalline with increased annealing temperature. Before annealing, the XRD pattern in Fig. 4-20 shows dominant Cu₂O (111) and Cu₂O (220) peaks. When the material is subjected to annealing at 300 °C, we can only see the traces of these Cu₂O peaks in Fig. 4-21 and upon subsequent increase of annealing temperature, these peaks fully disappear to give way to CuO peaks and becomes more crystalline. This result confirms the transformation of Cu/Cu₂O into CuO.

4.1.2.2 Effect of annealing temperature on grain size

In the case of laser ablation, the local temperature momentarily goes quite high and this favors the formation of Cu₂O from the ablated Cu and oxygen present in the water. The chemical reaction

$4\text{Cu} + \text{O}_2 \rightarrow 2\text{Cu}_2\text{O}$ requires only 1000 °C, which is adequately given by the laser pulse. In addition, the non reacting ablated Cu remains as is, in the water sample along with Cu₂O and this explains the presence of Cu and Cu₂O in the material before annealing (Jin, R et al 2012)As this material is filtered from the water and annealed in the atmosphere, cuprous oxide (Cu₂O) turns into cupric oxide (CuO) by the chemical reaction $2\text{Cu}_2\text{O} + \text{O}_2 \rightarrow 4\text{CuO}$ at about 300°C and CuO becomes more crystalline with the increase of temperature.

As expected, the XRD peaks of CuO narrow down with increasing temperature, indicating the growth of grain size. The grain size (D) of CuO nanoparticles at different annealing conditions was estimated using the familiar Scherrer formula $= \frac{k\lambda}{\beta \cos\theta}$. Where (β) is the full width at half maximum of diffraction peak, (θ) is the diffraction angle, (λ) is the X-ray wavelength and (k) is the Scherrer constant and its value is between 0.9 and 1. The estimated grain size is 9 ± 1 nm, 16 ± 1 nm and 26 ± 1 nm at 300°C, 600°C and 900°C respectively. It is well known that grain size increase due to the coalescence of small grains (agglomeration) or due to Ostwald ripening (thermal effect) (Ji, Z et al 2005) where the formation of larger particles is more energetically favored than smaller particles. This stems from the fact that molecules on the surface of a particle are energetically less stable than the ones already well ordered and packed in the interior. Large particles, with their lower surface to volume ratio, have a lower overall surface energy. Therefore, the number of smaller particles

continue to shrink while larger particles continue to grow in size (Imre, A et al 2000) The size of the CuO nanoparticles and their increased grain size, observed through the XRD data, are substantiated by the TEM images shown in Fig. 4-24, 4-25 and 4-26.

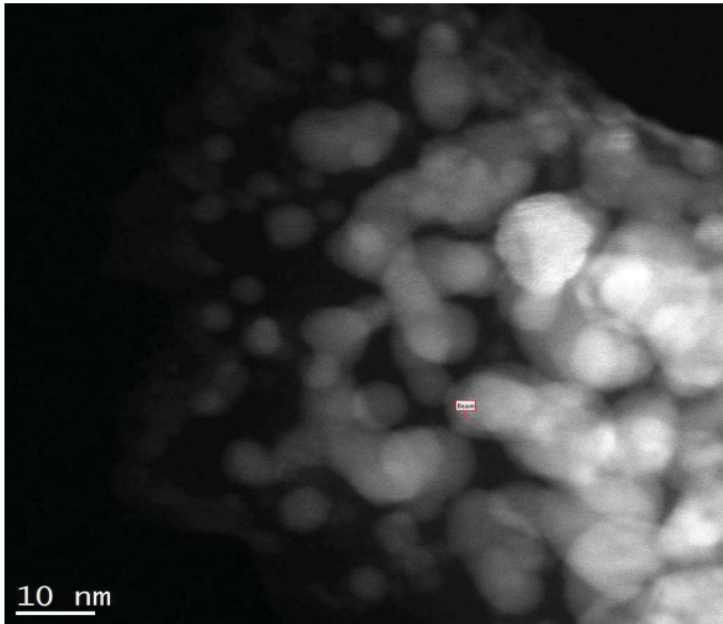


Fig 4-24 TEM image of unannealed Cu/Cu₂O sample.

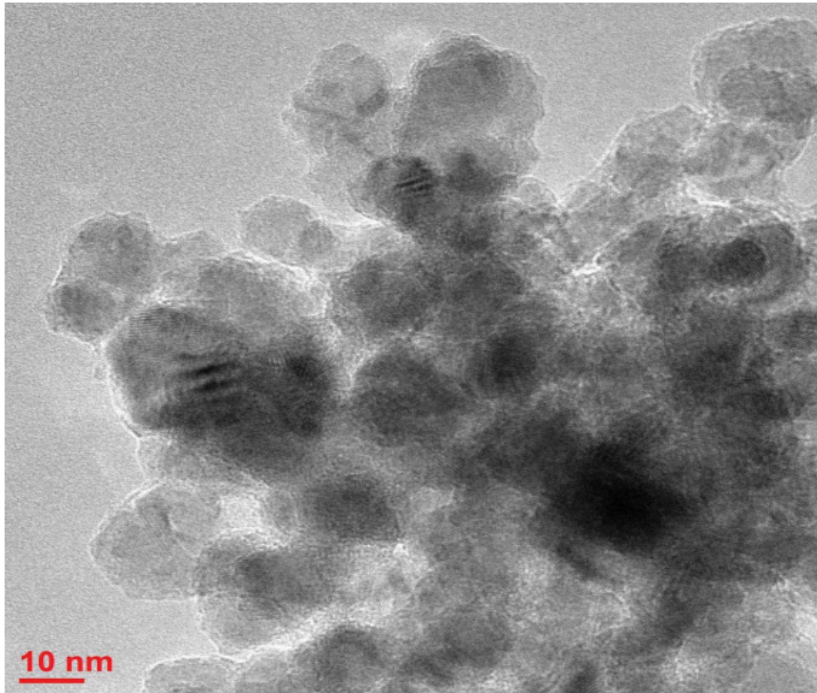


Fig 4-25 TEM image of annealed Cu/Cu₂O sample at 600°C.

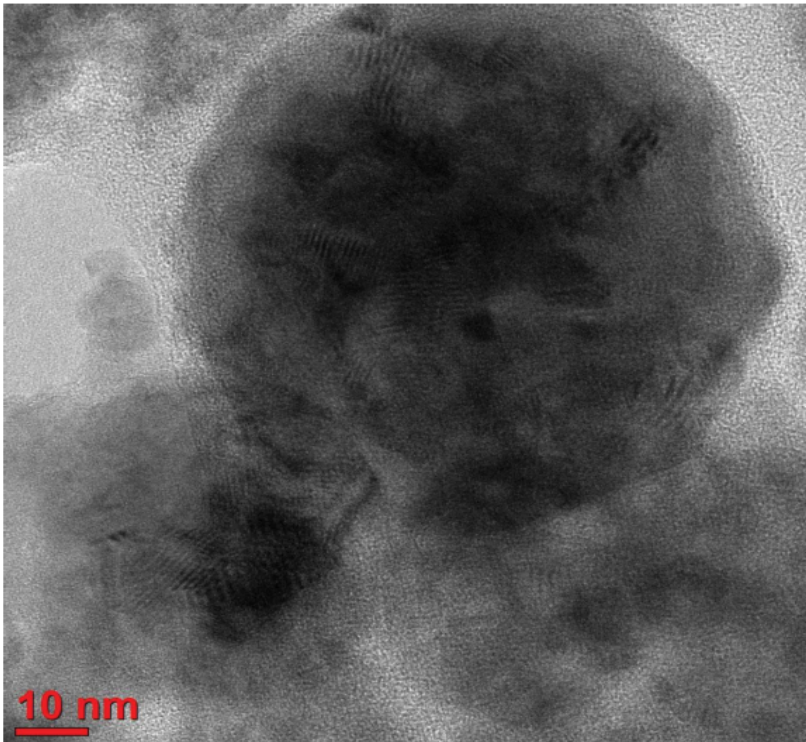


Fig 4-26 TEM image of annealed Cu/Cu₂O sample at 900°C.

4.1.2.3 Optical Characterization of unannealed/ annealed copper oxide NPs

In this section, we present the effect of annealing temperature on the optical characteristics of the synthesized material. The material as prepared, without any heat treatment (in the colloidal form) is used as a benchmark to study the variations in the optical characteristics with annealing temperature. The absorption spectrum of aqueous Cu/Cu₂O colloid as prepared is presented in Fig. 4-27 and the four peaks are marked at 641 nm, 335 nm, 274 nm and 217 nm. As mentioned in section 4.1.1.2, the broad peak (641 nm) is attributed to the surface plasmon resonance (SPR) of Cu (present in the prepared colloid). The weak absorption shoulders centered around 335 nm, 274 nm are due to the Brillouin transitions of cuprous oxide, whereas the highest peak (217 nm) in the spectrum is due to the inter-band transition of copper electrons close to the Fermi level.

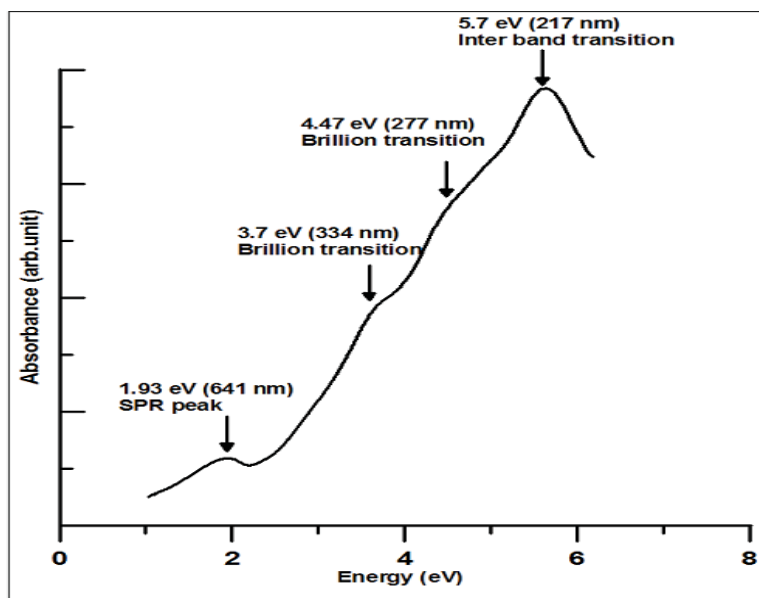


Fig 4-27 Absorption spectra of Cu/Cu₂O nanoparticles prepared by laser ablation of Copper in DW.

The band gap energy, the energy difference between the top of the valance band and the bottom of the conduction band, is an important characteristic of semiconducting material. For Direct Band gap material, plotting $(\alpha * E)^2$ vs. E linearises this relation. Hence, we can find the band gap energy of the material from the absorption coefficient (α) using Tauc plot. From the Tauc plot presented in Fig. 4-35, the band gap energy of Cu/Cu₂O is estimated to be 3.3 eV. The band gap energy of Cu/Cu₂O estimated from our work (3.3eV) is about 1 eV more than the

bulk
Cu₂O.

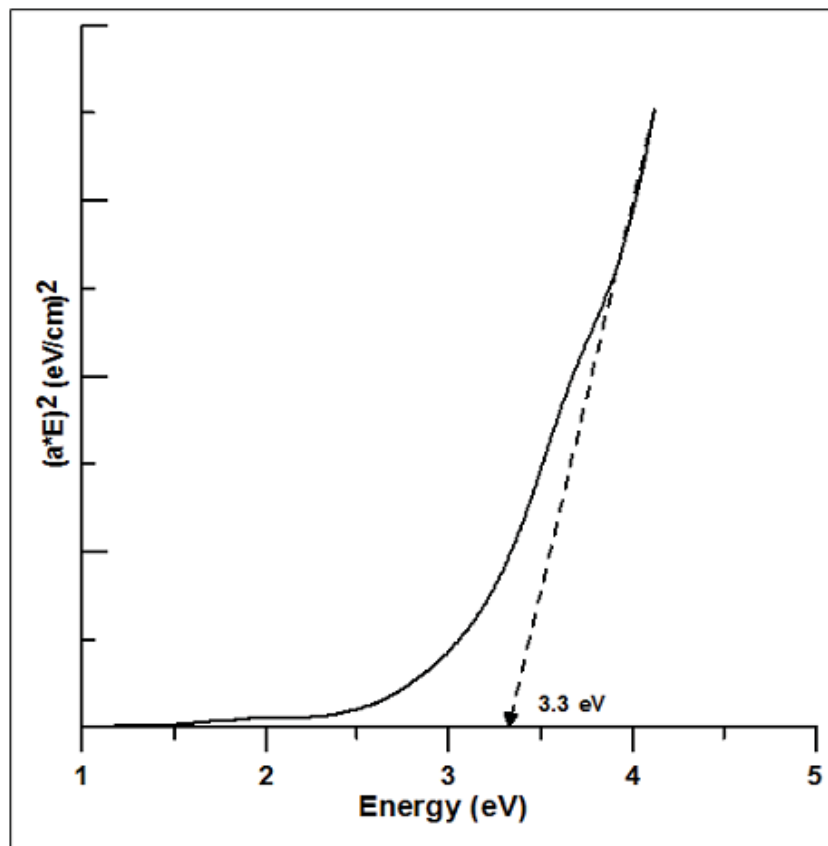


Fig 4-28 Tauc's plot of as-prepared material.

4.2 CONCLUSIONS

Pulsed laser Ablation in liquid using 532 nm wavelength laser having 10 Hz, 5 ns pulse duration was used to produce nanostructured copper oxide from copper in the presence of hydrogen peroxide (oxidizing agent) in aqueous solution. This brought about some positive attributes in the product material. First of all, the presence of H_2O_2 in the PLAL process favored the production of (Cu/CuO) with nanorod-like structure, which is more versatile in terms of its applications. Also the presence of H_2O_2 in the PLAL process made a considerable red shift in the band gap energy of the synthesized material, and reduced electron hole recombination rate as revealed by the photoluminescence spectra. The red shift in the band gap energy and the reduced electron hole recombination rate make the product material an ideal photo catalyst to harvest solar radiation.

In addition, we synthesized nano structured CuO by annealing Cu/Cu₂O at different temperatures via an indirect scheme. Cu/Cu₂O was synthesized by pulsed laser ablation of Cu in deionised water. Different techniques (XRD, TEM, UV spectrophotometry PL, and) were applied for the characterization of synthesized nanoCuO. The optical properties, grain size, band gap and IR absorption band of CuO vary with annealing temperature. The synthesized material using this indirect method could be applied in developing materials for sensors for various applications in industry, medicine and environment.

4.3 Recommendation

The pulsed laser ablation in liquid method of producing nano material is recommended as viable production technique given its superiority in terms of quality, cost and production rate as compared to the other approach.

References

- 1-Amikura, K, Kimura, T., Hamada, M., Yokoyama, N., Miyazaki, J. and Yamada, Y., 2008. Copper oxide particles produced by laser ablation in water. *Applied Surface Science*, 254(21), pp.6976-6982.
- 2- Ba, J.H. 2006. *Nonaqueous synthesis of metal oxide nanoparticles and their assembly into mesoporous materials* (Doctoral dissertation, Universität Potsdam Potsdam).
- 3-Chang, M.H. Liu, H.S. and Tai, C.Y., 2011. Preparation of copper oxide nanoparticles and its application in nanofluid. *Powder technology*, 207(1), pp.378-386.
- 4-Chowdhuri, A. Gupta, V. and Sreenivas, K., 2003. SENSING APPLICATIONS. *Rev. Adv. Mater. Sci*, 4, pp.75-78..
- 5-Devan, R.S., Patil, R.A., Lin, J.H. and Ma, Y.R., 2012. One-Dimensional Metal-Oxide Nanostructures: Recent Developments in Synthesis, Characterization, and Applications. *Advanced Functional Materials*, 22(16), pp 3326-3370.
- 6- El-Trass, A., ElShamy, H., El-Mehasseb, I. and El-Kemary, M., 2012. CuO nanoparticles: synthesis, characterization, optical properties and interaction with amino acids. *Applied Surface Science*, 258 (7), pp.2997-3001.
- 7-Feynman, R.P , 1961. Miniaturization *Reinhold, New York*, pp.282-296.
- 8- Fillot, F., Tókei, Z. and Beyer, G.P., 2007. Surface diffusion of copper on tantalum substrates by Ostwald ripening. *Surface science*, 601(4), pp.986-993.
- 9-Gopalakrishnan, K., Ramesh, C., Ragunathan, V. and Thamilselvan, M., 2012. Antibacterial activity of Cu₂O nanoparticles on E. coli synthesized from *Tridax procumbens* leaf extract and surface coating with polyaniline. *Digest Journal of Nanomaterials and Biostructures*, 7(2), pp.833-839.

- 10- Guha, S., Peebles, D. and Wieting, T.J., 1991. Zone-center ($q=0$) optical phonons in CuO studied by Raman and infrared spectroscopy. *Physical Review B*, 43(16), p.13092.
- 11- Heltemes, E.C., 1966. Far-Infrared Properties of Cuprous Oxide. *Physical Review*, 141(2), p.803
- 12- Hu, J.Q. and Bando, Y., 2003. Growth and optical properties of single-crystal tubular ZnO whiskers. *Applied Physics Letters*, 82(9), pp.1401-1403
- 13- Imre, A., Beke, D.L., Gontier-Moya, E., Szabo, I.A. and Gillet, E., 2000. Surface Ostwald ripening of Pd nanoparticles on the MgO (100) surface. *Applied Physics A*, 71(1), pp.19-22.
- 14- Jin, R., Gao, J., Liu, X., Yang, W., Peng, X., Zhang, T. and Zhou, Y., 2012. Ginsenoside Rg3: Spectral Analysis and Sensitive Detection with Silver Nanoparticles Decorated Graphene. *Science of Advanced Materials*, 4(11), pp.1160-1165.
- 15- Ji, Z., Zhao, S., Wang, C. and Liu, K., 2005. ZnO nanoparticle films prepared by oxidation of metallic zinc in H₂O₂ solution and subsequent process. *Materials Science and Engineering: B*, 117(1), pp.63-66.
- 16- Kawasaki, M., 2011. Laser-induced fragmentative decomposition of fine CuO powder in acetone as highly productive pathway to Cu and Cu₂O nanoparticles. *The Journal of Physical Chemistry C*, 115(12), pp.5165-5173.
- 17- Kelsall, R.W., Hamley, I.W. and Geoghegan, M. eds., 2005. *Nanoscale science and technology* (p. 108).
- 18- Kruis, F.E., Fissan, H. and Peled, A., 1998. Synthesis of nanoparticles in the gas phase for electronic, optical and magnetic applications—a review. *Journal of Aerosol Science*, 29(5), pp.511-535..
- 19- Lee, B.I., Qi, L. and Copeland, T., 2005. Nanoparticles for materials design: Present & future. *Journal of Ceramic Processing & Research*, 6(1), pp.31-40

- 20-Lee, J., Kim, D.K. and Kang, W., 2006. Preparation of Cu nanoparticles from Cu powder dispersed in 2-propanol by laser ablation. *Bull. Korean Chem. Soc*, 27(11), p.1869
- 21-Lee, M.T., Hwang, D.J., Greif, R. and Grigoropoulos, C.P., 2009. Nanocatalyst fabrication and the production of hydrogen by using photon energy. *international journal of hydrogen energy*, 34(4), pp.1835-1843.
- 22-Lin, X.Z., Liu, P., Yu, J.M. and Yang, G.W., 2009. Synthesis of CuO nanocrystals and sequential assembly of nanostructures with shape-dependent optical absorption upon laser ablation in liquid. *The Journal of Physical Chemistry C*, 113(40), pp.17543-17547.
- 23-Link, S. and El-Sayed, M.A., 1999. Size and temperature dependence of the plasmon absorption of colloidal gold nanoparticles. *The Journal of Physical Chemistry B*, 103(21), pp.4212-4217.
- 24-Liu, P., Cui, H., Wang, C.X. and Yang, G.W., 2010. From nanocrystal synthesis to functional nanostructure fabrication: laser ablation in liquid. *Physical Chemistry Chemical Physics*, 12(16), pp.3942-3952.
- 25-Mokerov, V.G., Fedorov, Y.V., Velikovski, L.E. and Scherbakova, M.Y., 2001. New quantum dot transistor. *Nanotechnology*, 12(4), p.552.
- 26-Momin, M.A., Pervin, R., Uddin, M.J., Khan, G.A. and Islam, M., 2010. One Step Synthesis and Optical Evaluation of Copper Oxide (CuO) Nanoparticles. *Journal of the Bangladesh Electronics Society*, 10(1-2).
- 27-Muniz-Miranda, M., Gellini, C. and Giorgetti, E., 2011. Surface-enhanced Raman scattering from copper nanoparticles obtained by laser ablation. *The Journal of Physical Chemistry C*, 115(12), pp.5021-5027.
- 28- Narang, S.N., Kartha, V.B. and Patel, N.D., 1992. Fourier transform infrared spectra and normal vibrations of CuO. *Physica C: Superconductivity*, 204(1-2), pp.8-14.
- 29- Nath, A. and Khare, A., 2011. Size induced structural modifications in copper oxide nanoparticles synthesized via laser ablation in liquids. *Journal of Applied Physics*, 110(4), p.043111.
- 30- Niu, K.Y., Yang, J., Kulinich, S.A., Sun, J., Li, H. and Du, X.W., 2010. Morphology control of nanostructures via surface reaction of

metallnanodroplets. *Journal of the American Chemical Society*, 132(28), pp.9814-9819.

31- Niu, K.Y., Yang, J., Kulinich, S.A., Sun, J. and Du, X.W., 2010. Hollow nanoparticles of metal oxides and sulfides: fast preparation via laser ablation in liquid. *Langmuir*, 26(22), pp.16652-16657.

32-Poole Jr, C.P. and Owens, F.J., 2003. *Introduction to nanotechnology*. John Wiley & Sons.

33-Rai, B.P., 1988. Cu₂O solar cells: a review. *Solar cells*, 25(3), pp.265-272

34-Ray, S.C., 2001. Preparation of copper oxide thin film by the sol-gel-like dip technique and study of their structural and optical properties. *Solar energy materials and solar cells*, 68(3), pp.307-312.

35-Singh, S.C., Zeng, H., Guo, C. and Cai, W., 2012. Lasers: Fundamentals, types, and operations. *Nanomaterials: Processing and Characterization with Lasers*, pp.1-34.

36-Taniguchi, N., 1974. On the basic concept of nano-technology Proceedings of the International Conference on Production Engineering Tokyo Part II Japan Society of Precision Engineering.

37-Yang, G.W., 2007. Laser ablation in liquids: applications in the synthesis of nanocrystals. *Progress in Materials Science*, 52(4), pp.648-698.

38-Yang, G. ed., 2012. Laser ablation in liquids: principles and applications in the preparation of nanomaterials. CRC Press.

39-Yan, Z. and Chrisey, D.B., 2012. Pulsed laser ablation in liquid for micro-/nanostructure generation. *Journal of Photochemistry and Photobiology C: Photochemistry Reviews*, 13(3), pp.204-223.

40-Yeh, M.S., Yang, Y.S., Lee, Y.P., Lee, H.F., Yeh, Y.H. and Yeh, C.S., 1999. Formation and characteristics of Cu colloids from CuO powder by laser irradiation in 2-propanol. *The Journal of Physical Chemistry B*, 103(33), pp.6851-6857

41-Yoon, K.H., Choi, W.J. and Kang, D.H., 2000. Photo-electrochemical properties of copper oxide thin films coated on an n-Si substrate. *Thin Solid Films*, 372(1), pp.250-256..